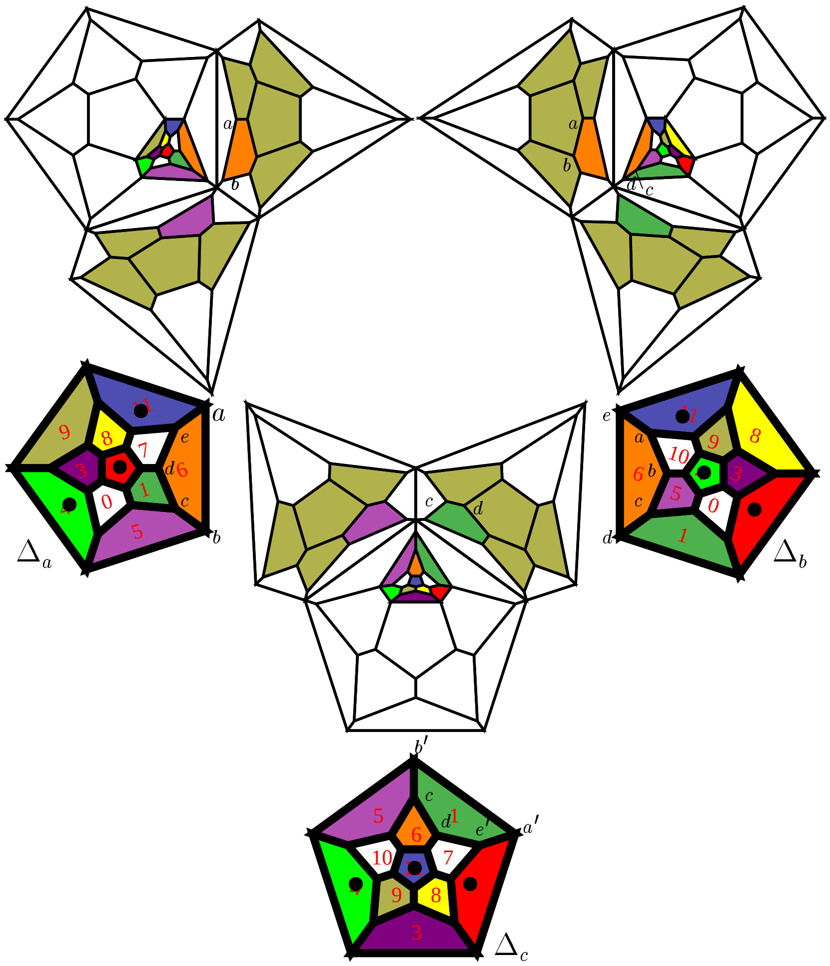

The tiling of the hyperbolic $4D$ space by the 120-cell is combinatoric

Maurice Margenstern

Publications du LITA, N° 2003-101

Service de reprographie de l'U.F.R. M.I.M., Université de Metz

Laboratoire d'Informatique Théorique et Appliquée, EA 3097 Université de Metz
Directeur de la publication : Maurice Margenstern

The tiling of the hyperbolic $4D$ space by the 120-cell is combinatoric

Maurice Margenstern

Université de Metz,
LITA, EA 3097, UFR MIM,
Île du Saulcy,
57045 Metz, France,
margens@lita.univ-metz.fr

Keywords: tilings, hyperbolic geometric, combinatorics, cellular automata.
Abstract The splitting method, which was defined by the author in [9, 10], is at the basis of the notion of combinatoric tilings. As a consequence of this notion, there is a recurrence sequence which allows us to compute the number of tiles which are at a fixed distance from a given tile. A polynomial is attached to the sequence as well as a language which can be used for implementing cellular automata on the tiling. We give here the polynomial and, as a first consequence, the language of the splitting is not regular, as it is the case in the tiling of hyperbolic $3D$ space by rectangular dodecahedra which is also combinatoric.

1 Introduction

Starting from a certain time, several papers appeared which, more or less, claimed that they belong to a combinatoric approach to hyperbolic geometry.

In 1999, in a workshop of **FCT** on **Formal Languages and Automata**, I presented a paper which was a joint work with Kenichi Morita, see [11, 12], which was an implicit application of the splitting method. Indeed, the method which I just devised had not yet a name, but it was already applied. But this was only the geometrical aspect of the method. It had an algebraic side which I found a bit later and which was first explained in [6]. During a certain time, it was called the *Fibonacci technology.* Several applications were done after that and only recently I clearly stated a definition from which all the previous theorems appear as various illustrative examples of the scope of the method.

The goal of this paper is to prove the following theorem:

Theorem 1 – *The tiling of* $\mathbb{H}^4$ *which is built on the* 120*-cell by tessellation is combinatoric,*

where the notion of a *combinatoric tiling* is defined in the section 2 of this paper.

Recall that a tiling is obtained by **tessellation** from some polyhedron P of the space if and only if its tiles are exactly obtained by reflecting P in its hyper-faces and, recursively, its successive images in their hyper-faces.

In the second section, we explain the splitting method, in particular, indicating what is a combinatoric tiling.

In the third section we recall the minimal notions of hyperbolic geometric which are needed in order to understand the paper. In the fourth section, as a first step of the proof, we revisit the construction of the 120-cell which is mandatory in order to understand the splitting which is the concern of the fifth section. In the sixth section, we deal with the polynomial and the language of the splitting which gives us a new piece of information to the theorem 1:

Theorem 2 − *The language of the splitting which is associated to the tiling of $I\!H^4$ which is built on the* 120*-cell by tessellation is not regular. The greatest real root of the polynomial of the splitting is a Perron number.*

2 The splitting method

2.1 The geometric side

The method is based on the notion of a **basis of splitting** which was introduced in [10]. Such a basis consists in two finite families of closed, simply connected sets of the considered geometric space X. The sets are also supposed to be with a non-empty interior. The sets of the first family, say $S_0, \ldots, S_n$ are called **regions** and they are assumed to be unbounded. The sets of the second family, say, $P_0, \ldots, P_k$ are called the **generating tiles** and they are bounded. Moreover, these two families of sets have the following properties:

(i) X splits into finitely many copies of S_0,

(ii) any S_i splits into one copy of some P_ℓ and finitely many copies of S_j's,

where **copy** means an **isometric image**, and where, in the condition (ii), the copies may be of different S_j's, S_i being possibly included.

As usual, it is assumed that the interiors of the copies of the $\mathcal{P}_\ell$'s and the copies of the S_j's which are involved are pairwise disjoint.

The set S_0 is called the **head** of the basis.

Consider a basis of splitting of X, if any. We recursively define a tree A which is associated with the basis as follows. First, we split S_0 according to the condition (ii) of the above definition. This gives us a copy of say P_0 which we call the **root** of A and which we call also the **leading tile** of S_0. The root constitutes the 0^{th} generation and S_0 is the region of the 0^{th} generation. Assume that $S_{n_1}, \ldots, S_{n_{m_n}}$ are all the regions of the n^{th} generation. By definition, their **leading tiles**, the copy of P_ℓ in the condition (ii), constitute the nodes of the n^{th} generation. We split these S_j's according to the condition (ii). We obtain m_n tiles which are called the tiles of the $n{+}1^{\text{th}}$ generation and, for each S_{n_h} which is some S_i, we have a splitting which is the isometric image of the splitting of S_i as it is above indicated. Call the leading tiles of these copies of the splitting of S_i the *sons* of the leading tile of S_{n_h}. By definition, the sons of the leading tile of S_{n_h} belong to the $n{+}1^{\text{th}}$ generation. The union of all the sons of the nodes of the n^{th} generation constitutes the nodes of the $n{+}1^{\text{th}}$ generation.

This recursive process shows that A is an infinite tree with finite branching. We call A the **spanning tree of the splitting**, where the splitting refers to the basis of splitting $S_0, \ldots, S_k$.

Definition 1 – *Say that a tiling of X is* **combinatoric** *if it has a basis of splitting and if the spanning tree of the splitting yields exactly the restriction of the tiling to S_0, where S_0 is the head of the basis.*

An illustrative example is given by the splitting of $I\!H^2$, the hyperbolic plane, which generates the pentagrid, the tiling $\{5,4\}$ in Schläfli notations, *i.e.* five sides and an interior angle of $\dfrac{\pi}{2}$. See the figure 1, in the section 3.

Definition 2 – *Say that a tiling is* **quasi-combinatoric** *if it has a sub-tiling which is combinatoric.*

Recall that a **sub-tiling** of a tiling is a partition of the same set where the members of the partition are unions of tiles of the initial tiling. We also can view a sub-tiling as a partition over the partition which is defined by the tiling.

From the definition of a combinatoric tiling, it is not difficult to see that a sub-tiling of a tiling $\mathcal{T}$ is generated by **super-tiles** which split into finitely many tiles of $\mathcal{T}$.

In this paper, we consider only the case when we have a single generating tile, *i.e.* when $h = 1$.

2.2 The algebraic side

The splitting method has also algebraic consequences. From [9], we know that when a tiling is combinatoric, there is a polynomial which is attached to the spanning tree of the splitting.

More precisely, we have the following result:

Lemma 1 – (Margenstern, [9]) *Let $\mathcal{T}$ be a combinatoric tiling, and denote a basis of splitting for $\mathcal{T}$ by S_0, …, S_k with $P_0, \ldots, P_h$ as its generating tiles. Let $\mathcal{A}$ be the spanning tree of the splitting. Let M be the square matrix with coefficients m_{ij} such that m_{ij} is the number of copies of S_{j-1} which enter the splitting of S_{i-1} in the condition (ii) of the definition of a basis of splitting. Then the number of nodes of $\mathcal{A}$ of the n^{th} generation are given by the sum of the coefficients of the first row of M^n. More generally, the number of nodes of the n^{th} generation in the tree which is constructed as $\mathcal{A}$ but which* *is rooted in a node being associated to S_i is the sum of the coefficients of the $i+1^{\text{th}}$ row of M^n.*

This matrix is called the **matrix of the splitting** and we call **polynomial of the splitting** the characteristic polynomial of this matrix, being possibly divided by the greatest power of X which it contains as a factor. Denote the polynomial by P. From P, we easily infer a recurrence equation which allows us to compute very easily the number u_n of nodes of the n^{th} level of $\mathcal{A}$. This gives us also the number of nodes of each kind at this level by the coefficients of M^n on the first row: we use the same equation with different initial values. The sequence $\{u_n\}_{n\in\mathbb{N}}$ is called the **recurrent sequence of the splitting**.

First, as in [6, 9], number the nodes of $\mathcal{A}$ level by level, starting from the root and, on each level, from left to right. Second, consider the recurrent sequence of the splitting, $\{u_n\}_{n\geq 1}$: it is generated by the polynomial of the splitting. As we shall see, it turns out that the polynomial has a greatest real root β and that $\beta > 1$. The sequence $\{u_n\}_{n\geq 1}$ is increasing. Now, it is possible to represent any positive number n in the form $n = \sum\limits_{i=0}^{k} a_i.u_i$, where $a_i \in \{0..\lfloor\beta\rfloor\}$, see [3], for instance. The string $a_k \dots a_0$ is called a representation of n. In general, the representation is not unique and it is made unique by an additional condition: we take the representation which is maximal with respect to the lexicographic order on the words on $\{0..b\}$ where $b = \lfloor\beta\rfloor$. The set of these representations is called the **language of the splitting**.

Although this notion was introduced in order to study tilings of hyperbolic spaces, it may apply also in the euclidean case or other situations of unbounded manifolds. The notion was successfully applied to various tilings of hyperbolic spaces, mainly $\mathbb{H}^2$ and $\mathbb{H}^3$, the hyperbolic $3D$ space, see [6, 7, 8, 13, 14, 15, 16, 17]. We turn now to the proof that the method also applies to $\mathbb{H}^4$ with the tiling being based on the 120-cell.

3 Recalling some features of hyperbolic geometry

3.1 About hyperbolic geometry

We refer the reader to [18] for introductory material on hyperbolic geometry. In order to make the paper as self-contained as possible and also to spare space for this paper, we shall use Poincaré's disk model of the hyperbolic plane, see Figure 1, below, and its natural generalizations to higher dimensions.

The open unit disk U of the euclidean plane constitutes the points of the hyperbolic plane $\mathbb{H}^2$. The border of U, ∂U is called the set of *points at infinity*. Lines are the traces in U of its diameters or the traces in U of circles which are orthogonal to ∂U. The model has a very remarkable property, which it shares with the half -plane model: hyperbolic angles between lines are the euclidean angles between the corresponding circles.

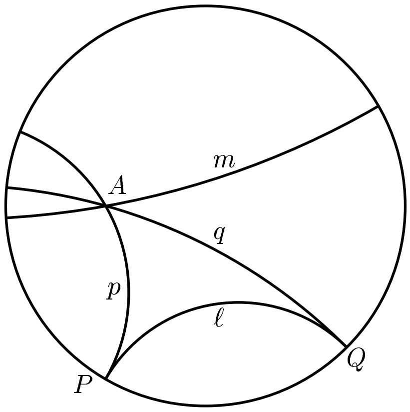

Figure 1. The Poincaré model of $I\!H^2$

In order that the reader could be more familiarised to the hyperbolic geometry and in order to illustrate the splitting method by a concrete example, we give in the figure 2 the application of the method to the pentagrid which is the tiling being obtained by the tessellation of the rectangular regular pentagon.

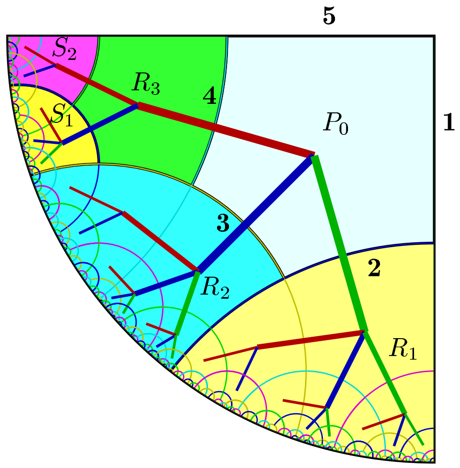

Figure 2. The splitting of $\mathcal{Q}$ which is associated to the pentagrid. Notice the construction of the spanning tree.

The model is easily generalised to higher dimension: in [14, 15], it is done for $I\!H^3$, where the hyperbolic $3D$ space is the interior of the unit ball of $I\!R^3$. The planes are the trace in the ball of spheres which are orthogonal to the unit sphere, diametral planes being considered as a limit case. Lines are intersections of planes.

As a model of the hyperbolic $4D$ space, we take the interior of the unit ball of $I\!R^4$. Hyper-planes are the traces in the ball of hyper-spheres which are orthogonal to the unit sphere, diametral hyper-planes being a limit case. Planes are intersections of hyper-planes and lines are intersections of planes.

3.2 The incidence properties of $4D$ spaces.

In order to better understand the constructions of the paper, it is appropriate to remember some basic features of the $4D$ spaces. In particular, what we need further is the incidence number of vertices, edges, faces and hyper-faces with respect to one another.

Indeed, this is easy to establish from the following remark: as the classical hyper-spherical model is a conformal image of the hyperbolic $4D$ space, it is also *locally* homeomorphic to $I\!E^4$. In particular, we get the needed information if we look at what happens for a hypercube, *i.e.* $[0,1]^4$ around one of its vertices, say the point O with coordinates $(0,0,0,0)$. Around O, there are exactly 16 hyper-cubes. All of them are defined by the following formula: $\prod\limits_{i=0}^{3}(-1)^{\epsilon_i}.[0,1]$, where $\epsilon_i \in \{0,1\}$ and $(-1).[0{,}1] = [-1{,}0]$ and, of course, $1.[0{,}1] = [0{,}1]$.

Consider how many hyper-cubes go through a given cube. We may decide that the cube is $C = \{0\}\times[0,1]^3$. And so, there are exactly two hyper-cubes which contain C, $[0,1]^4$ and $[-1,0]\times[0,1]^3$. They are symmetric with respect to C and, also, $[0,1]^4$ is the image of $[-1,0]\times[0,1]^3$ under the shift along the line through O and $(1,0,0,0)$ which transforms O in the latter point. Now, consider a *face* $F = \{0\}\times\{0\}\times[0,1]^2$. There are four hyper-cubes which pass through F. They are of the form $(-1)^{\epsilon_0}.[0,1]\times(-1)^{\epsilon_1}.[0,1]\times[0,1]^2$. We see at the same time that there are also four cubes which pass through F. We have indeed two pairs of symmetric cubes with respect to F. The first pair is given by $(-1)^{\epsilon_0}.[0,1]\times\{0\}\times[0,1]^2$ and the second one is given by $\{0\}\times(-1)^{\epsilon_1}.[0,1]\times[0,1]^2$. If we impose to the cubes to be in the hyper-cube $[0,1]^4$, we obtain two cubes: those where $\epsilon_i = 0$ in the previous formulas.

We apply the same argument in order to get the hyper-cubes, cubes and faces which pass through a given edge, for instance $\{0\}\times\{0\}\times\{0\}\times[0,1]$. In $I\!E^4$, we have, respectively, 8 hyper-cubes, 12 cubes and 6 faces, and in the hyper-cube $[0,1]^4$, we have, respectively 6 cubes and 3 faces. Indeed, if we consider the cubes, for instance, we have three families, depending on the position of the vertex component: first, $(-1)^{\epsilon_0}.[0,1]\times(-1)^{\epsilon_1}.[0,1]\times\{0\}\times[0,1]$, then $(-1)^{\epsilon_0}.[0,1]\times\{0\}\times(-1)^{\epsilon_1}.[0,1]\times[0,1]$, with the vertex in the middle and, at last: $\{0\}\times(-1)^{\epsilon_0}.[0,1]\times(-1)^{\epsilon_1}\times[0,1]$. We know that in the case of $[0,1]^4$, the objects for which we are looking are given by $\epsilon_i = 0$.

The same argument for a vertex gives us 16 hyper-cubes, 32 cubes, 12 faces and 8 edges in $\mathbb{E}^4$ and 1 hyper-cube, 4 cubes, 6 faces and 4 edges in the hyper-cube $[0,1]^4$.

We can sum up this information in the following two tables which, according to the above indicated local homeomorphism, hold also for, respectively, $\mathbb{H}^4$ and the 120-cell:

	0	1	2	3
1	8			
2	12	6		
3	32	12	4	
4	16	8	4	2

	0	1	2
1	4		
2	6	3	
3	4	3	2

Table 1. The tables of incidence in $\mathbb{H}^4$ and in the 120-cell.

3.3 Interior and exterior of the 120-cell

One of the problems to deal with the $4D$ geometry, is that in several regards, the views are misleading. Indeed, most of the views which are used in order to represent $4D$ objects are $2D$ projections. Even if we can see these $2D$ figures in the $3D$ space, the projection induces a distortion and it cannot give an account of a deep property of the $4D$ space: it is possible to turn around a plane without touching it. This is a generalisation of an analogous property in lower dimension: we can turn around a point in the plane and around a line in the $3D$ space. On the other hand, we cannot turn around a point in a line, around a line in a plane, around a plane in the $3D$ space and around a hyper-plane in the $4D$ space.

A hyper-face of the 120-cell defines a hyper-plane which splits $\mathbb{H}^4$ in two half-spaces. Each hyper-face has also the property that one of the half-spaces which it defines contains all the 120-cell while the other contains of it only the hyper-face. Generalising what is trivial for $\mathbb{H}^2$ and for $\mathbb{H}^3$, call the **interior side** of a hyper-face $\mathcal{F}$ of the 120-cell, the open half-space being determined by $\mathcal{F}$ which intersects the 120-cell. The **interior** of the 120-cell is the intersection of all the interior sides which are defined by its hyper-faces. By *abus de langage*, we will also call **interior** of the 120-cell the union of the 120-cell itself with its interior in the preceding meaning.

4 Revisiting the construction of the 120-cell

It is difficult to represent the 120-cell. A lot of papers are devoted to this point, and the reader is referred to [20, 1, 19], for more details on this topic.

4.1 Schlegel diagrams

In this paper, we shall make use of another tool, a very old one, which is also used in [19]: **Schlegel diagrams**.

The Schlegel diagram of a figure F in a $3D$ space, either euclidean, elliptic or hyperbolic, is the central projection of F on a plane, starting from a particularly chosen point of the space. For more details on these diagrams, see for instance, [19, 2, 4]. Such a representation takes place in the euclidean plane but, as already indicated, it can be used for the study of $3D$ spaces, whatever the geometry is.

The same tool can be used for $4D$ space, either euclidean, elliptic or hyperbolic, as it is done in [19]. Indeed, we make use of $3D$ projections from which we take the Schlegel diagram.

Recall that in $I\!H^4$, as in the other hyperbolic spaces, whatever the dimension is, there are no similitude. Consequently, all 120-cells of $I\!H^4$ are isometric. And so, in this sense, there is a single 120-cell from the point of view of the Schlegel diagram. A global view of the 120-cell does not allow us to grasp it from an algorithmic point of view. On the opposite, local views are worth of interest and will allow us to prove that the tiling which is based on the tessellation of the 120-cell is combinatoric.

The 120-cell is constituted by 120 rectangular dodecahedra which obeys the characteristic being given by the Schläfli symbol of the corresponding tiling: $\{5, 3, 3, 4\}$. This means that the $2D$-faces are regular rectangular pentagons, that the $3D$-faces are regular rectangular dodecahedra, that any edge is shared by three dodecahedra and that any vertex is shared by four dodecahedra. We already know all this information from the incidence tables 1.

In the next subsections, we give an account of the construction thanks to the Schlegel diagrams. This construction will help us to define the splitting, which is the goal of the fifth section.

4.2 Notations and conventions.

The initial, or 0^{th} generation is given by a dodecahedron which can be represented as indicated in the figure 3.

The figure represents a true Schlegel diagram of a dodecahedron. In this figure, we numbered the sides of the dodecahedron from 0 up to 11. The face 0 does not appear directly: it is the 'hidden face' which is bordered by the faces 1 up to 5.

Notice that all the elements of the dodecahedron can be identified thanks to the numbering of the faces. As edges are shared by two faces, we can number each one by the two numbers of the faces in which they appear. In the same way, as vertices are shared by three faces, we can number each vertex by the three numbers of the faces for which it is a common point.

We give names to the faces of the dodecahedron which are easier to remember than numbers and which imply an orientation which is also easy to define. Below, the table 2 list all of them.

We can also enumerate the faces, the edges and the vertices in several **rings**. This enumeration is represented by the table 2. It works as follows. We go from the outer part of the figure downto its center, going clockwise.

0	back	4	side	8	leg
1	shoulder	5	shoulder	9	leg
2	side	6	head	10	hand
3	feet	7	hand	11	stomach

Table 2. The correspondence between names and numbers.

Notice that in many places we shall also call the stomach **the top**.

For the faces, we have two faces: the back and the stomach each one constituting a singleton. Then, we have two rings, the **outer ring** with the faces from 1 up to 5 and the **inner ring** with the faces from 6 up to 10. The outer ring is around the back and the inner ring is around the stomach.

For the edges, we distinguish five rings which we number from I up to V. The table 3 gives the list of these edges. The ring I contains the **outer edges** of the dodecahedron which are the sides of the face 0 and the ring V contains the sides of the face 11.

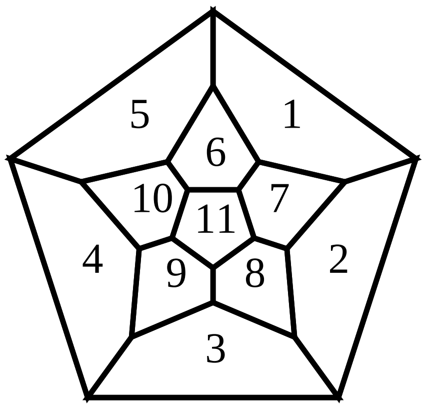

Figure 3. The 0^{th} generation

At last, the vertices are also displayed in four rings being numbered from I up to IV. The numbers of the vertices of each ring is given by the table 3.

The table 3 will allow us to control the construction of the 120-cell by counting the new elements which appear in the process. The right hand part of the table 1 will also be an important help to control the correctness of the process. We shall, refer to these tables as to the **incidence tables** and it will always be clear from the context, whether we consider the incidences within the 120-cell or in $I\!H^4$.

4.3 The first generation.

Our construction will rely on purely combinatorics considerations and we shall see that they are enough in order to obtain an algorithmic representation of the 120-cell which leads us to the splitting of the corresponding tiling.

As traditionally, for the first generation, we put a dodecahedron on each face of the dodecahedron Δ of the 0^{th} generation, perpendicularly to Δ. We have to describe this carefully. At each vertex of Δ, three edges meet which are pairwise perpendicular. And so there is a single direction which is orthogonal to the already existing edges. Two points can be chosen in this direction. Once we chose one of them for a given vertex say V, it fixes the construction: the new dodecahedra which will be constructed on the faces of Δ which share V will also share the chosen new point. This also consists in choosing one of the two half-spaces being defined by the hyperplane which is generated by the dodecahedron. Once we constructed the first dodecahedron, say $\mathcal{D}_0$ on a face of Δ, Δ intersects one of the half-spaces being generated by $\mathcal{D}_0$ and not the other. As $\mathcal{D}_0$ is a hyper-face of the considered 120-cell, what will be its interior intersects Δ. This defines the interior of $\mathcal{D}_0$. Now, the construction of the other dodecahedron shares the same property. And so, their interior is determined by the half-space which they generate and which meets the already constructed hyper-faces. We shall say that the new dodecahedra are constructed by the **orthogonal completion** and when it will be needed, we shall add: **with respect to** Δ.

For this generation, we denote the new dodecahedra by an index which corresponds to the faces of Δ: D_0, D_1, ..., D_{11}. For the numbering of the faces of each D_i, we proceed as previously. In order to fix the numbering without ambiguity, it is enough to fix which is the face 1 of each dodecahedron and then, using the clockwise orientation of the diagram, we obtain the numbering of the other faces. The face 1 is fixed to its turn by its topmost outer vertex, say the **initial point**: (5,0,1) in the dodecahedron of the figure 3.

The table 4 gives us the correspondence between the dodecahedra and their initial point.

Using self-explanatory notions, consider now the faces $[D_5](2)$ and $[D_6](5)$, *i.e.* the left shoulder of D_5 and the right one of D_6. They share the edge (5,6) of Δ. As an edge is shared by exactly three dodecahedra, we have that the just considered faces are identical. And so, we have to mark all the identifications which occur in the diagram. This is done in the figure 4, below.

faces	
back	0
outer ring	1, 2, 3, 4, 5
inner ring	6, 7, 8, 9, 10
top	11

edges	
ring I	(0,1), (0,2), (0,3), (0,4), (0,5)
ring II	(1,2), (2,3), (3,4), (4,5), (5,1)
ring III	(1,6), (1,7), (2,7), (2,8), (3,8) (3,9), (4,9), (4,10), (5,10), (5,6)
ring IV	(6,7), (7,8), (8,9), (9,10), (10,6)
ring V	(11,6), (11,7), (11,8), (11,9), (11,10)

vertices	
ring I	(0,5,1), (0,1,2), (0,2,3), (0,3,4), (0,4,5)
ring II	(5,1,6), (1,7,2), (2,8,3), (3,9,4), (4,10,5)
ring III	(6,1,7), (7,2,8), (8,3,9), (9,4,10), (10,5,6)
ring IV	(11,6,7), (11,7,8), (11,8,9), (11,9,10), (11,10,6)

Table 3. The rings of faces, edges and vertices.

D_1	(1,5,0)	D_5	(1,5,0)	D_9	(10,11,9)
D_2	(1,0,2)	D_6	(5,1,6)	D_{10}	(5,6,10)
D_3	(9,8,3)	D_7	(6,7,1)	D_{11}	(10,6,11)
D_4	(5,4,0)	D_8	(11,7,8)	D_0	(1,5,0)

Table 4. The topmost vertex of the dodecahedra of the first generation.

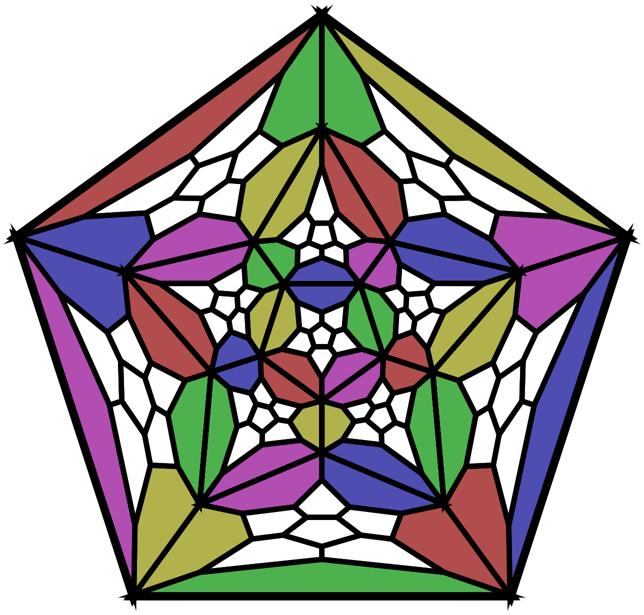

Figure 4. The 1^{st} generation and its identifications

We obtain that we remain with 72 faces which are not covered. Before turning to the second generation, we have to count the new elements which are brought in by the dodecahedra of the first generation.

From the figure 4, we notice that we have 12 'independent' zones which remain after the previous identifications. All white face have to be counted once. However, the identified faces do exist in the 120-cell as we know from the incidence table: they were not present in the previous generation, and so we have also to count them. But, as we see in the figure 4, each face of this kind appears twice. On another hand, the back of the dodecahedra of the first generation have not to be counted: they are the faces of Δ.

We sum up this information on the left hand part of the table 5, where the label of each row indicates how many times the elements being indicated are counted. We do not indicate the elements which are not counted as already being counted in the previous generation. As we have 12 zones, this means that the number of new faces is $12\times(\dfrac{5}{2}+5+1) = 102$.

We apply the same principle for the edges.

We first notice that the ring I belongs to the back of all the considered dodecahedra: they where already counted. The edges of the ring II are shared by three dodecahedra and so, they are counted three times. For example, in the figure 4, the reader can easily be convinced that the edges $[D_5](1,2)$, $[D_6](5,1)$ and $[D_1](4,1)$ are the same: consider the identifications of the coloured faces which contain them. The edges of the ring III are shared by two dodecahedra and so, they are counted twice. See, for instance, the edges $[D_5](1,6)$ and $[D_1](4,5)$ of the figure 4. On another hand, the edges of the rings IV and V are new ones and all of them must be counted once. This gives us $12\times(\frac{5}{3}+\frac{10}{2}+5+5)=$ 200 new edges. At last, we perform the same computation for the vertices.

As previously, and for the same reason, the ring I is ruled out as being already counted by the previous generation. The vertices of the ring II belong to edges of the ring II and so they are also counted three times. The vertices of the ring III, which belong to edges of the ring III are thus counted twice. Only the vertices of the ring IV are new ones. And so, we obtain: $12\times(\frac{5}{3}+\frac{5}{2}+5)$=110 new vertices.

	low	up	top	II	III	IV	V	II	III	IV
1		5	1			5	5			5
2	5				10				5	
3				5				5		

Table 5. Counting the contribution of the first generation to the new elements of the 120-cell at the considered stage of the process.

The label which is at the beginning of a row is the multiplicity of the elements of the row.

4.4 The second generation.

Consider an 'independent' zone of the figure 4. It consists in the inner ring of faces of the considered dodecahedron with its top. Let us put a dodecahedron on each face of the inner ring by the orthogonal completion. Assume that such a dodecahedron is put on the face $[D_5](7)$, so that we shall denote it $D_{[5](7)}$. Notice that $[D_5](7,1)$ is an edge of this face which is also shared by D_1. As an edge belongs exactly to three dodecahedra, this means that the dodecahedron $D_{[5](7)}$ is identical to the dodecahedron $D_{[1](10)}$. But $[D_5](7,2)$ is an edge of $D_{[5](7)}$ which is also shared by D_6 and so, by a similar argument, we obtain that $D_{[5](7)}$ is identical to $D_{[6](6)}$.

And so, if by the orthogonal completion we put a dodecahedron on each inner face of the dodecahedra of the first generation, the same dodecahedron is counted three times. Accordingly, we obtain 20 new dodecahedra which we shall call of the second generation.

This property of of three copies for the same dodecahedron is due to the distortion which is introduced by the Schlegel diagram. However, the Schlegel diagram will help us: the three copies are taken from *different points of view* and this property will allow us to obtain the further information by only combinatoric means.

Indeed, let us look at the dodecahedron $D_{[5](7)}$. We have three images of it: $D_{[5](7)}$, $D_{[1](10)}$ and $D_{[6](6)}$.

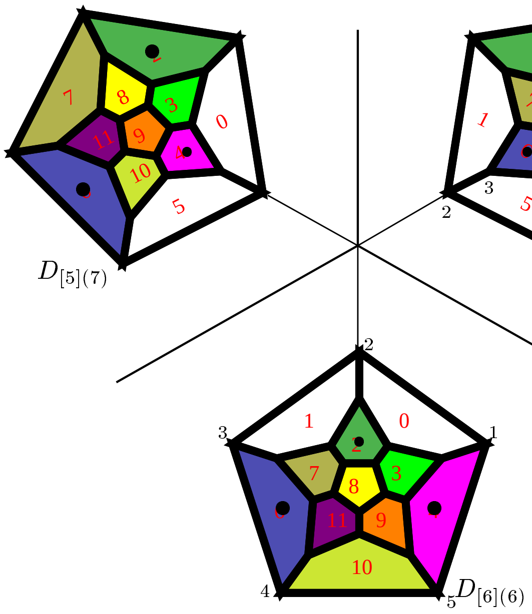

Figure 5. The 2nd generation in the Schlegel diagram:
the colours represent corresponding faces
a dotted face is counted twice
notice the numbering of corresponding faces.

In the figure 5, we represent $D_{[5](7)}$, $D_{[1](10)}$ and $D_{[6](6)}$ which are different views of the same dodecahedron. We give a different colour to each face, except for the faces which are already counted and which we coloured in white. In order to make the correspondence completely, we also number the faces of this dodecahedron. We give the standard numbering to $[D_{[1](10)}$, using the table 4, and we show on the figure 5 where are the numbers on the other views of $[D_{[1](10)}$. For each view, consider that the feet are opposite to the common vertex of the three views. It fixes their local numbering which is different from the numbering of the identification, except for $D_{[1](10)}$. Notice that the face $[D_{[5](7)}](1)$ is the back of $D_{[6](6)}$ and that, similarly, $[D_{[5](7)}](5)$ is the back of $D_{[1](10)}$ while $[D_{[1](10)}](1)$ is the back of $D_{[5](7)}$ and $[D_{[1](10)}](5)$ is the back of $D_{[6](6)}$, that $[D_{[6](6)}](5)$ is the back of $D_{[5](7)}$ and $[D_{[6](6)}](1)$ is the back of $D_{[1](10)}$. Notice that the labelling of the vertices of $[D_{[1](10)}](5)$ in the figure 5 and the corresponding numbering on the back of $D_{[6](6)}$ helps us to make the correspondence of all the other faces.

It is now possible to count the new elements which are the contribution of the second generation. This counting is given in the table 6. This time, as some elements of higher rank appear to be already counted, we indicate the multiplicity 0 in the table 6 and in the following ones.

For the faces, we know that two faces of the outer ring are already counted from the previous generation: they share a face with the previous generation. In the outer ring, two faces are counted twice: as an example, the face 4 of $D_{[5](7)}$ is shared by $D_{[5](8)}$. All the faces which are shared by another dodecahedron which is not represented in the figure 5 are indicated by a dot in this figure. Notice that such a face appears as an inner face in another view of $D_{[5](7)}$. And so, on the inner ring, we have also one face which is counted twice. And so, we remain with a single new face in the outer ring and four ones in the inner ring. The top is also a new face.

For the edges, we have already three sides which belong to the ring II. As the remaining ones belong to faces which are counted twice, they are also counted twice. The incidence of the already counted faces explains the counting which is displayed by the table 6. The same observation applies to the vertices, of course. We obtain 150 new faces, 270 new edges and 140 new vertices.

	low	up	top	II	III	IV	V	II	III	IV
0	2			3	4			3	2	
1	1	4	1		2	3	4		1	3
2	2	1		2	4	2	1	2	2	2

Table 6. Counting the contribution of the second generation to the new elements of the 120-cell at the considered stage of the process.
The label which is at the beginning of a row is the multiplicity of the elements of the row.

4.5 The third generation.

The second generation was obtained by putting dodecahedra on the inner faces of the dodecahedra of the first generation according to the orthogonal completion. As a consequence, the corresponding tops remain free. There are twelve of them. For the third generation, we put one dodecahedron on the tops of the dodecahedra of the first generation. This contributes with 12 dodecahedra to the hyper-faces of the 120-cell. Also, starting from this generation, all the elements of the first generation are completely covered.

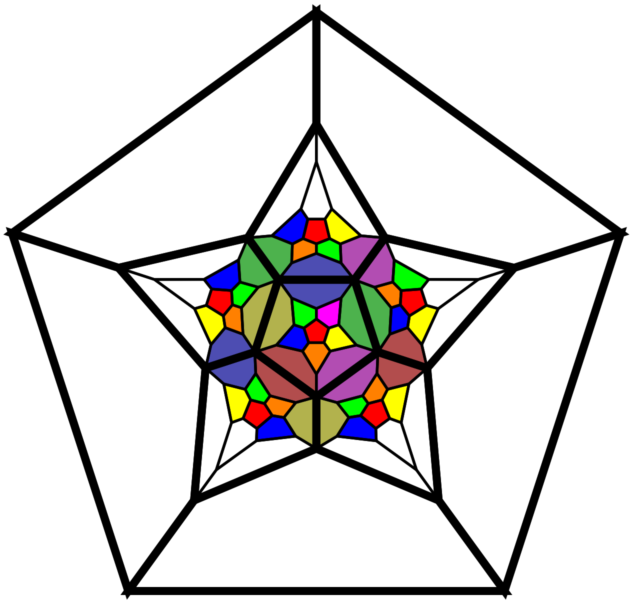

Figure 6. Partial view on the 3rd generation:
The faces which are in white are already covered

	low	up	top	II	III	IV	V	II	III	IV
0	5			5	10			5	5	
1		5	1			5	5			5

Table 7. Counting the contribution of the third generation to the new elements of the 120-cell at the considered stage of the process.
The label which is at the beginning of a row is the multiplicity of the elements of the row.

Above, the figure 6 displays a zone which comes from the first generation. The outer ring is constituted by faces of the dodecahedra of the first generation which are identified. The inner ring shows dodecahedra of the second generation. Notice that four faces of each dodecahedron of the second generation are now covered. On the top, we have a dodecahedron of the third generation.

The figure shows the identification of faces between the second and the third generation: the feet of each dodecahedron of the second generation which are displayed in the figure 6 are identified with an outer face of the dodecahedron of the third generation being represented.

From the picture and from the study of the second generation, we obtain that the whole outer ring has the 0 multiplicity. The inner ring and the top are new faces. We infer the consequences for the edges and then for the vertices: these are easy details which are left to the reader. Accordingly, there are 72 new faces, 120 new edges and 60 new vertices.

4.6 The fourth generation.

As all faces of the first generation are covered, we put a dodecahedron on each face of the upper ring of each dodecahedron of the third generation, observing the orthogonal completion.

On the figure 7, we give two adjacent faces of the first generation. The outer ring is white and it contains no Schlegel diagram: the face is identified with another one of the same generation. On the inner ring, each face contains a Schlegel diagram: it represents the dodecahedron of the second generation which was put there by the orthogonal completion. At last, on the top face of the dodecahedron of the first generation, there is also a Schlegel diagram: the dodecahedron of the third generation which was put there. We also take into account the identification of faces which results from the study of the second and third generations: the feet of a dodecahedron of the second generation is an outer face of a dodecahedron of the third one. Also, some faces of the outer and inner rings of the second generation are identified with other faces of the second generation. This explains the white faces of the figure 7: they are completed faces which do not appear when we are at the stage of the fourth generation.

Notice the six dotted faces of the figure 7: one of them belongs to the upper dodecahedron D^* of the third generation, another one to the lower dodecahedron D_* of the third generation also. Another dotted face belongs to the dodecahedron D^*_ℓ of the second generation which is on the left side of D^*. Similarly, another dotted face belongs to the dodecahedron D^ℓ_* of the second generation which is on the left side of D_* in the figure. We define D^*_r and D^r_* for the two remaining dotted faces in a similar way. Notice that D^*_ℓ and D^ℓ_* are identical but are represented by different views on the figure 7. In particular, the dotted face of D^*_ℓ is adjacent to the feet of this dodecahedron. It is the same for the dotted face of D^ℓ_*. But, the other face of D^*_ℓ which is adjacent to both the feet of this dodecahedron and its feet appears as the top face in D^ℓ_*.

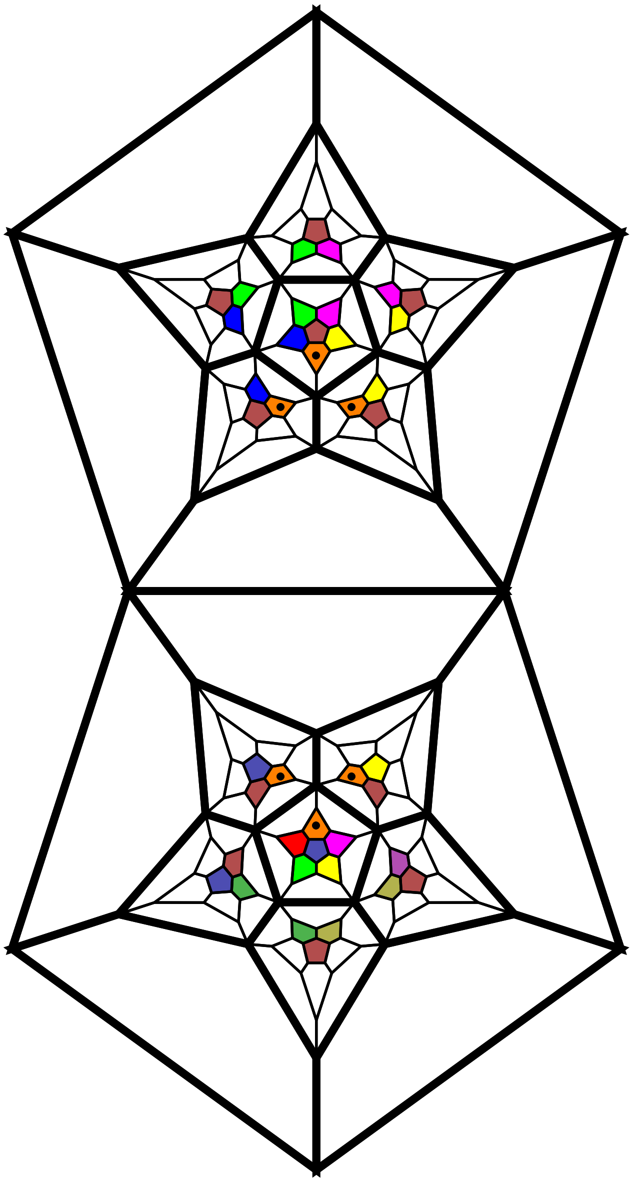

Figure 7. Locating the dodecahedra of the 4$^{\text{th}}$ generation:
The faces which are in white are already covered

The dotted faces of the figure 7 belong to the same dodecahedron of the fourth generation: indeed the sides of the dotted face of D^* which belong to the ring III of D^* are identical with the corresponding sides of the dotted face of D_*. This means that before the fourth generation, these edges are already shared by two different dodecahedra. As they are also shared by the dodecahedra which are put on the dotted faces, these dodecahedra are identical.

The remark which we indicated about the inner faces of D_ℓ^* which are adjacent to its feet shows that the dodecahedra of the fourth generation are pairwise distinct. We represent this fact in the figure by displaying the colours of the inner faces and the top of D^* in a different way as in D_*. And so, there is no other identification of the dodecahedra which we introduced.

Summing up our considerations, we obtain that each dodecahedron which we introduced is identified to exactly another one: to the nearest one of that generation in the Schlegel diagram. Accordingly, there are 30 dodecahedra in the fourth generation.

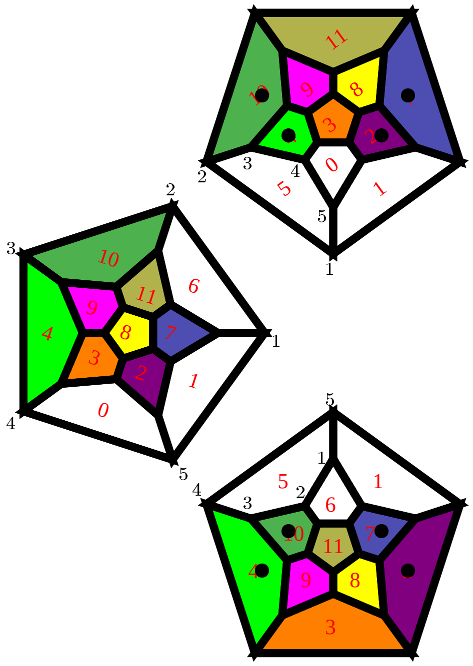

Figure 8. The 4^{th} generation in the Schlegel diagram:
the colours represent corresponding faces
dotted faces are counted twice
notice the numbering in order to establish a correct correspondence

In order to count the new elements, we have now to look closer at the two views of the same dodecahedron of the fourth generation. As an auxiliary tool, we shall use the view of the dodecahedron D° being constructed on the dotted face in D_ℓ^*. Notice that this view is the same as the view of that dodecahedron which is obtained on the dotted face of D_*^ℓ. This is why we need only three views in the figure 8 which represent the views of the same dodecahedron of the fourth generation.

In the figure 8, we use the same 'trick' as in the figure 5 in order to establish the correspondence of the faces by colouring and numbering the same faces in the same hue and with the same number. By looking carefully on the figure 7, we can see that the vertex being numbered 5 in D^* is not 'symmetric' to its position in D_*. The displacement from D^*_ℓ to D^ℓ_* induces this kind of shift in the positions.

These views allow us to establish the counting of the new elements. The counting is displayed in the table 8 which makes use of the same conventions as the previous tables.

For the faces, we see that three are already counted on each dodecahedron: two ones in the outer ring and a single one in the inner ring. Due to the respective positions of the dodecahedra on the inner faces of a dodecahedron of the second generation, the sides of the dodecahedra of the fourth generation are shared by two dodecahedra of this generation. And so, they are counted twice. The figure 8 shows us that these outer faces appear as inner faces in the other view of the dodecahedron. And so, these faces are counted twice.

Applying these consideration to edges and vertices, we obtain the counting which is given by the table 8. In the figure 8, notice that there is an edge which is shared by two dotted faces: accordingly, such an edge is shared by three dodecahedra, and so it is counted three times. The reader may check that we get 180 faces, 290 edges and 140 vertices.

	low	up	top	II	III	IV	V	II	III	IV
0	2	1		3	4	2	1	3	2	2
1	1	2	1		2	1	2		1	1
2	2	2		2	2	2	2	2		2
3					2				2	

Table 8. Counting the contribution of the fourth generation to the new elements of the 120-cell at the considered stage of the process.
The label which is at the beginning of a row is the multiplicity of the elements of the row.

4.7 The fifth generation.

Looking again at the figure 7, we notice that the fourth generation was obtained by putting a dodecahedron on each inner face of the dodecahedra of the third generation by the orthogonal completion. Accordingly, at the present moment, the top of the dodecahedra of the fifth generation are still free. And so, we put a dodecahedron on each top of the dodecahedra of the third generation. This provides us with 12 additional dodecahedra: the dodecahedra of the fifth generation. It is easy to notice that, as in the case of the third generation, these dodecahedra are 'independent' from each other. Notice also that from now on, the dodecahedra of the third generation are covered. The situation of these dodecahedra looks very much the situation which is described by the figure 8, with this difference that we are now by one 'circle' deeper in the structure of the 120-cell. The figure 9 indicates the place of this dodecahedron with respect to the dodecahedron of the first generation from which it comes. Clearly, at this stage, a rather global figure is of no use. In order to see better, we have to go back to the third generation and see how things look now, starting from that point.

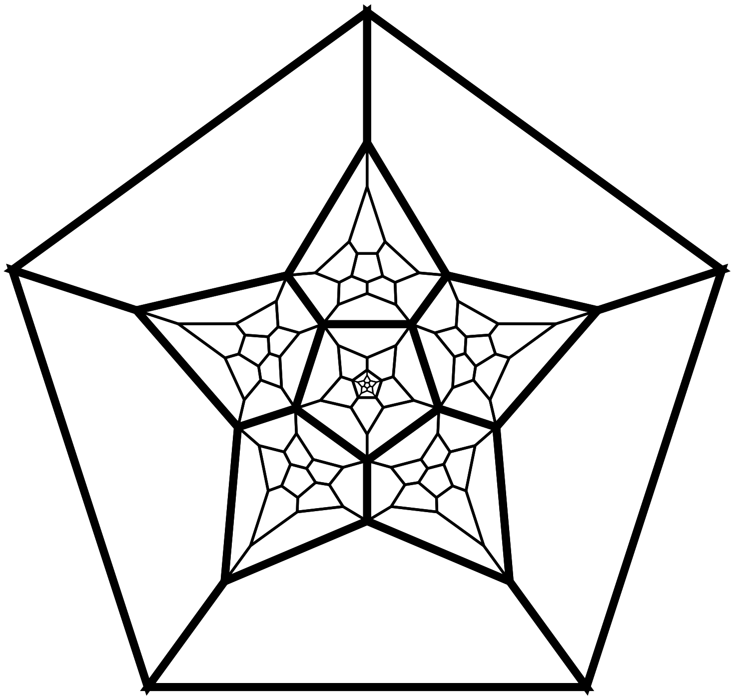

Figure 9. The 5^{th} generation in the Schlegel diagram:
a very partial view

As a dodecahedron of the fifth generation is in the top face of a dodecahedron of the third generation and as each face of the inner ring supports a dodecahedron of the fourth generation, the feet of the dodecahedra of the fourth generation are shared by a face of the inner ring of a dodecahedron of the fifth generation.

And so, for the counting of the new elements, we obtain a table which looks very much the same as the table for the third generation:

	low	up	top	II	III	IV	V	II	III	IV
0	5			5	10			5	5	
1		5	1			5	5			5

Table 9. Counting the contribution of the fifth generation to the new elements of the 120-cell at the considered stage of the process.

And so, in particular, we obtain 72 new faces, 120 new edges and 60 new vertices.

4.8 The sixth generation.

Now that we covered completely the third generation, we put one dodecahedron on each inner face of the dodecahedra of the fifth generation according to the orthogonal completion. we have to look closer at the situation. Taking into account the figure 9, we obtain the figure 10, see below.

The figure 10 allows us to see better the location of the new dodecahedra. Roman letters indicate the generation of some dodecahedra from which it is easy to infer the generation of each dodecahedron of the figure.

Recall that the fourth and fifth generations are put on the inner faces and on the top of the third generation, respectively. The identification of the faces between the fourth and the fifth generation make it clear that the faces which are indicated in orange inside of each dodecahedron of the third generation in the figure 10 belong to the same dodecahedron of the sixth generation which is put on the orange inner face of the dodecahedron of the fifth generation. Now, the identifications between the blue dodecahedra of the fourth generation from one hand and the identifications between the green ones and between the purple ones make it clear that the three orange faces of the fifth generation which we indicate in the figure 10 belong to the same dodecahedron of the sixth generation. This shows that such dodecahedra are counted three times and so there are 20 of them.

And so, the Schlegel diagram gives us three different views for the same dodecahedron of the sixth generation. Let us make a zoom on each triple which consists in a dodecahedron of the fifth generation and two ones of the fourth generation.

We shall use the same method as for the fourth generation, namely, by using the numbering of the vertices of a face which is shared by a dodecahedron of the fourth generation. The correspondence which we already studied between the two views of the dodecahedra of the fourth generation allows us to translate the numbering from one view to the other one. The figure 11 illustrates this point. In order to make the checking easier, there are two zooms of the same triple of identical dodecahedra of the sixth generation, say Δ_a, Δ_b and Δ_c. For each Δ_λ, the global zoom shows us its place on the dodecahedron of the fifth generation which shares a face with it and the two neighbouring dodecahedra of the fourth generation.

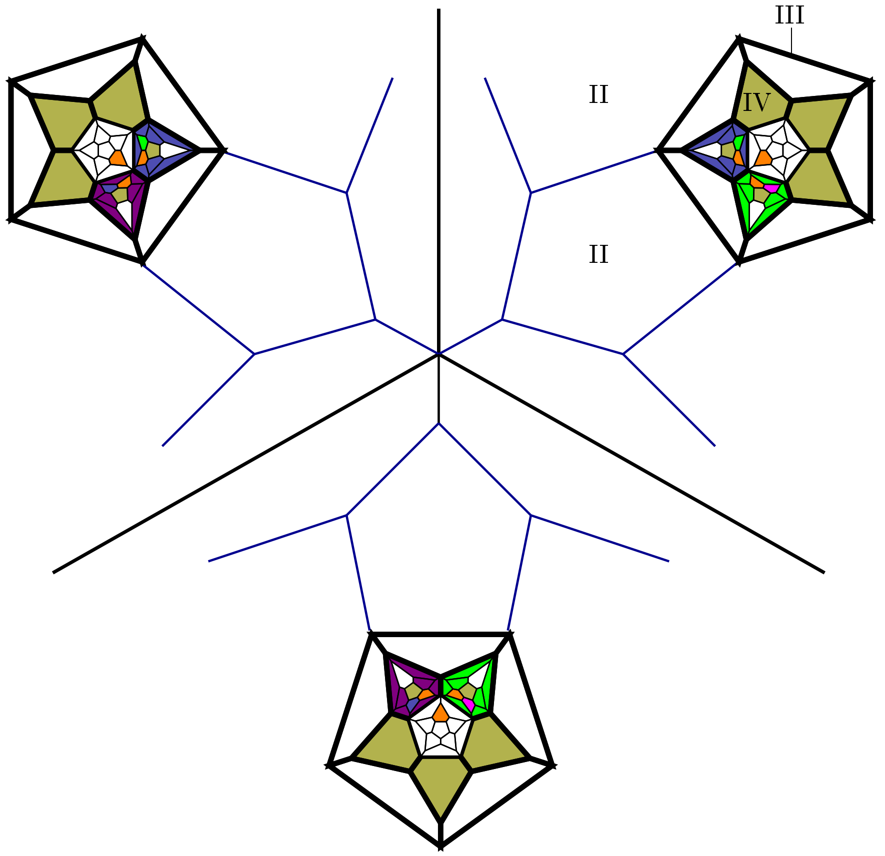

Figure 10. The location of the 6^{th} generation in the Schlegel diagram: The roman letters indicate the generation which can easily be propagated.
In orange, in the face of the fifth generation, the same dodecahedron of the sixth generation

On the figure 10, we noticed that Δ_λ shares a face with two dodecahedra of the fourth generation. Taking into account the observations which we already made, we conclude that now, all faces of the fourth generation are also covered: this is clear as far as the legs were the only not yet covered faces. Indeed, the stomach of a view of the fourth generation is identified with the feet of the other view of the same dodecahedron.

There is a second zoom which focuses on the sixth generation only. Each Δ_λ is represented at a greater scale below the global zoom of the situation of its neighbouring.

And so, we have the correspondence which is provided by the figure 11. The figure also allows us to detect the faces which are already belonging to a previous generation. This is the case for faces which are in contact with a face of the fourth generation. If we take as a reference the view Δ_c for which the numbering of the faces is self-explanatory, we notice that the faces 1 and 5 are in this case. But from the other views, we notice that the face 1 is the face 6, *i.e.* the head, of another view. It is not difficult to see also that the face 0 of Δ_c, is the face 10 of Δ_b, *i.e.* the left hand of Δ_c, and that the face 7 of Δ_b, *i.e. the right hand* of Δ_b, is the face 0 of Δ_a. And so, the faces which are already present are the faces 0, 1, 5, 6, 7 and 10.

The same figure also allows us to detect the faces which are counted twice. This is of course the case for the faces 2 and 4 of Δ_c. By the identifications between the three views, we conclude that the face 11 is also counted twice, as it appears as the face 4 of Δ_a, *i.e.* the left side of Δ_a. This allows us to infer the counting of the edges and then, of the vertices.

It is now possible to count the new elements with which the sixth generation contributes to the construction of the 120-cell. It is not difficult to see that this time there are no elements which are counted three times and so, we obtain 90 new faces, 120 new edges and 50 new vertices. The table 10 gives all the elements of this counting.

	low	up	top	II	III	IV	V	II	III	IV
0	2	3		3	6	4	3	3	4	4
1	1	2			2	1			1	
2	2		1	2	2		2	2		1

Table 10. Counting the contribution of the sixth generation to the new elements of the 120-cell at the considered stage of the process.

4.9 The seventh generation.

As the fourth generation is completely covered and as for the fifth one we covered only the inner faces, the top faces of the dodecahedra of the fifth generation remain free.

And so, we put a dodecahedron on the top of each dodecahedron of the fifth generation according to the orthogonal completion. This produces 12 new dodecahedra.

The figure 12 represents such a dodecahedron in its surrounding within the Schlegel diagram. We notice the triples of faces around a vertex, two faces belonging to neighbouring dodecahedra of the sixth generation and the third face belonging to the dodecahedron of the seventh one. And so there is room for a dodecahedron there. But it is another dodecahedron of the seventh generation.

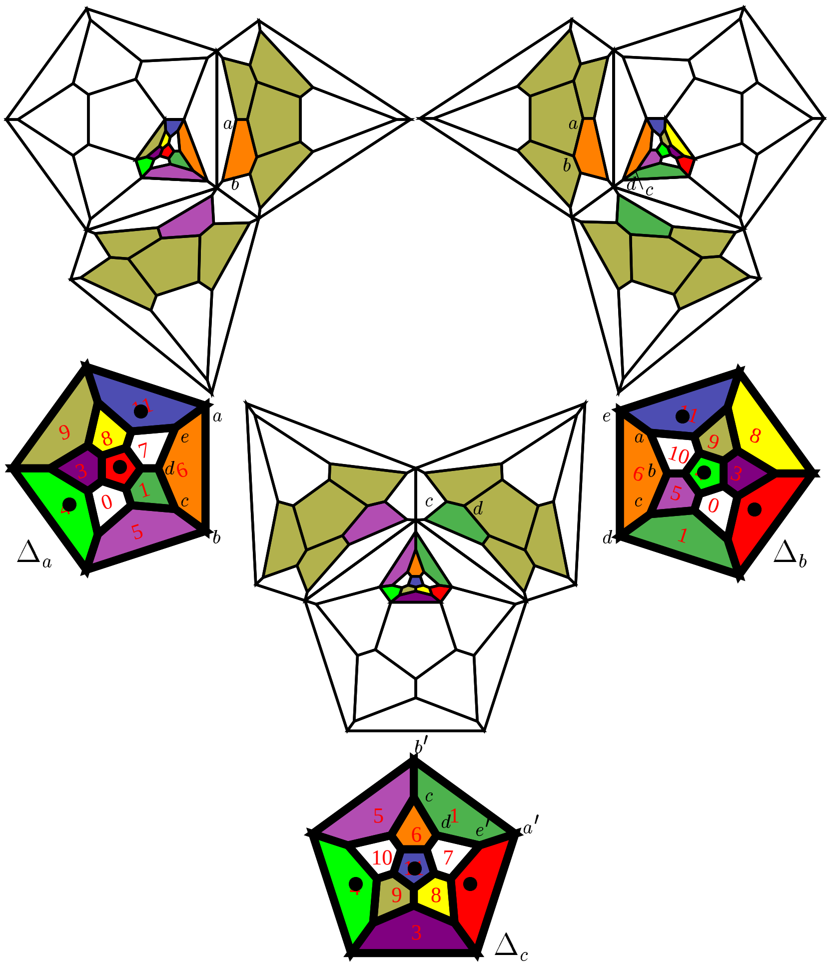

Figure 11. The 6^{th} generation in the Schlegel diagram:
superposition of two different zooms:
dotted faces are counted twice
notice the numberings in order to establish
a correct correspondence

Indeed, let Δ_a^*, Δ_b^* and Δ_c^* be the dodecahedra of the seventh generation which are adjacent, respectively, to Δ_a, Δ_b and Δ_c from the figure 11. We see that Δ_a^* shares a face with Δ_a which is the feet of Δ_a. But we know that Δ_a is identical to Δ_b. But the foot of Δ_a is a leg in Δ_b and in Δ_c. This means that the dodecahedron which touches Δ_b by its leg and Δ_b^* by the face which is in the above considered triple is exactly Δ_a^*. Notice also that this configuration shows that $\Delta_a^* \neq \Delta_b^*$. Accordingly, all the faces of the inner ring of a dodecahedron of the seventh generation are counted twice.

As we have edges which are shared by faces being counted twice, these edges are counted three times. It is also the same for the vertices which belong to such edges. This explains the account which is displayed by the table 11. And so, we obtain 42 new faces, 50 new edges and 20 vertices.

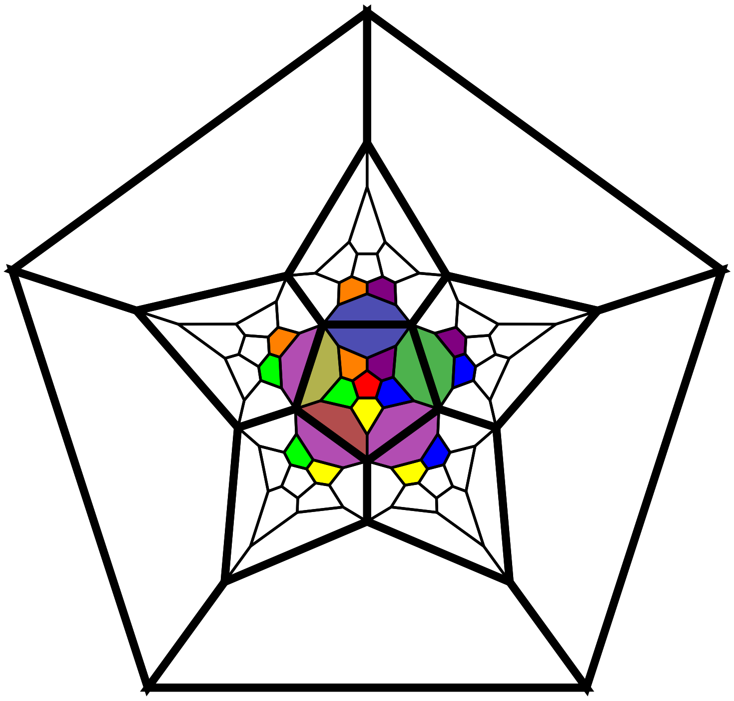

Figure 12. The 7^{th} generation in the Schlegel diagram: for the dodecahedra of the 6^{th} generation, we colour only the faces which are free before the insertion of the 7^{th} generation

	low	up	top	II	III	IV	V	II	III	IV
0	5			5	10			5	5	
1			1							
2		5					5			
3						5				5

Table 11. Counting the contribution of the seventh generation to the new elements of the 120-cell at the considered stage of the process.

4.10 The eighth generation.

Now, we see that all the faces of the sixth generation are covered and there is a single face remaining free on each dodecahedron of the seventh generation, all the other faces being covered. And so, if we put a dodecahedron on one of these free faces according to the orthogonal completion, this dodecahedron must touch the other ones as far as it cannot touch any face which is already covered. And so, there is a single dodecahedron of the eighth generation. But there is a more convincing argument.

Consider the three faces of the sixth generation which were free before appending the dodecahedra of the seventh generation. We represent all of them in the figure 13 with the same colour being given to the three views of the same face. Also, in order to locate the face more easily, we number the faces of Δ_a, Δ_b and Δ_c, giving the same number to the corresponding faces, as we already did in the analyses for the previous generations. Recall that the numbering of Δ_c is the standard one and that the place of the corresponding faces do not coincide with their standard numbering in Δ_a and Δ_b. Indeed, we defined the standard numbering with respect to the feet of the corresponding views which, by our convention, is the face of these dodecahedra of the sixth generation which are in contact with a dodecahedron of the seventh generation. In order to avoid confusions, when we shall use the number of a face, we shall add the precision whether it is under the identification or under the standard numbering.

In order to locate the faces of Δ_a^*, Δ_b^* and Δ_c^*, we also number them and here we adopt the standard numbering: the feet of these views is the face with which they touch the corresponding dodecahedron of the sixth generation, see the figure 13. Accordingly, the feet of Δ_c and Δ_c^* receive the same number 3, but the feet of Δ_a^* which are numbered by 3 touch the face of Δ_a which is numbered by 9 in the identification. Similarly, the feet of Δ_b^* which are also numbered by 3 touch the face of Δ_b which is numbered by 8 in the identification.

Consider now the face 8 in the identification between Δ_a, Δ_b and Δ_c. It is the left hand leg of Δ_a, being standardly numbered 9, the feet of Δ_b being standardly numbered 3 and the right hand leg of Δ_c, also being standardly numbered 8. Now, if we put a dodecahedron on that face 8 of Δ_a under the identification, this dodecahedron is identical to Δ_b^*. Now, the edge (8,9) of Δ_a under the identification cannot be shared by more than three dodecahedra. This edge is also the edge (3,9) of Δ_b^*. As an edge is at most shared by three dodecahedra, we have that Δ_a^*, Δ_a and Δ_b^*, which are pairwise distinct, share this side. As the face 3 of Δ_b^* is identified with the face 9 of Δ_a in the identification, necessarily, the face 9 of Δ_b^* must be identified to the face 8 of Δ_a^*. In this process the edges (8,9) of Δ_a^* and Δ_b^* are identified. As a consequence, the edge (8,11) of Δ_a^* is identified with the side (9,11) of Δ_b^*. And so, the tops of Δ_a^* and Δ_b^* have a common edge. As these tops are faces of different dodecahedra, if we put another dodecahedron on one of them by the orthogonal completion, it will also share this side and, consequently, the other face. Notice that, by the same argument, we can identify the face 8 of Δ_b^* with the face 9 of Δ_c^* and the face 9 of Δ_a^* with the face 8 of Δ_c^*. In the figure, the edge (9,11) of Δ_a^* is identified with the edge (8,11) of Δ_c^* and the edge (8,11) of Δ_b^* is identified with the edge (9,11) of Δ_c^*. Accordingly, the twelve tops of the seventh generation belong to a single dodecahedron which is the single one of the eighth generation.

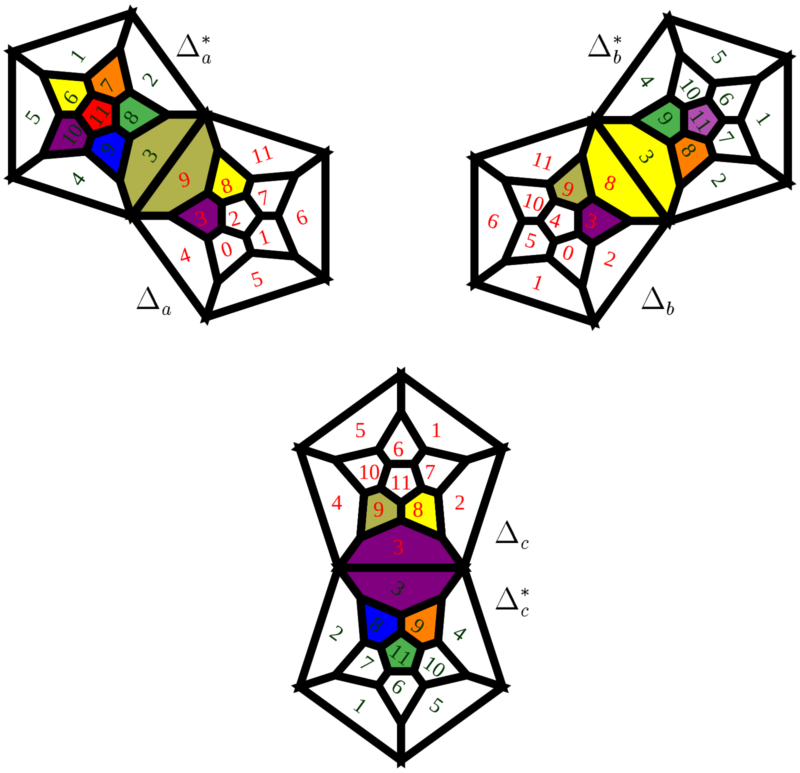

Figure 13. The 7^{th} generation in the Schlegel diagram:
superposition of two different zooms:
dotted faces are counted twice
notice the numberings in order to establish
a correct correspondence

It is now clear that all the other elements of the dodecahedron of the eighth generation are already present in the dodecahedra of the seventh one. Accordingly, the eighth generation contributes with no new face, nor new edge nor new vertex to the construction of the 120-cell. Indeed, the dodecahedron of the eighth generation completes the construction: when the seventh generation was completed, there was room only for just one dodecahedron.

Instead of a table of the contribution of the eighth generation, below, we display a table which sums up the contribution of each generation and gives us the well known amount of dodecahedra, faces, edges and vertices of the 120-cell: see the table 12.

generation	dodecahedra	faces	edges	vertices
0	1	12	30	20
I	12	102	200	110
II	20	150	270	140
III	12	72	120	60
IV	30	180	290	140
V	12	72	120	60
VI	20	90	120	50
VII	12	42	50	20
VIII	1	0	0	0
total	120	720	1200	600

Table 12. General counting of all the contributions to the elements of the 120-cell for each generation.

5 The splitting of $I\!H^4$

5.1 General tools

For this splitting, we shall use again the Schlegel diagrams. However, their use will be more complex than what was done by the author in [14, 15].

The first thing which we have to see, is how to define the splitting and how to represent it in the Schlegel diagram.

Starting from this point, the term *dodecahedron* stands for *rectangular regular* dodecahedron.

The basic point is that the first region S_0 is a sixteenth of $I\!H^4$, *i.e.* the intersection of the half-spaces which are determined by four pairwise perpendicular hyper-planes. Call this region a **hyper-corner**. We fix a 120-cell $\mathcal{M}_0$ at the extremal point O of S_0, which belongs to all the hyper-planes which generated S_0, and we notice that this hyper-corner can be represented by the four dodecahedra of the 120-cell $\mathcal{M}_0$ which meet at O. As by definition they are pairwise perpendicular and as each one generates a $3D$ hyperbolic space, we can easily reconstruct the hyper-corner from $\mathcal{M}_0$, once we fix one of its vertices: from the incidence table 1, we know that precisely four dodecahedra meet in the vertex and, moreover, they are pairwise perpendicular. Our problem is now to split the complement of $\mathcal{M}_0$ in S_0.

Let $\mathcal{D}_0, \mathcal{D}_1, \mathcal{D}_2$ and $\mathcal{D}_3$ these four dodecahedra. Their respective positions at a vertex, one with respect to each other, are symmetric. This can be checked on the hyper-cube around a vertex, as we remarked in the subsection 3.2. And so, we have to remind this symmetry of positions, even if we give names which, up to a point, break this symmetry. Call $\mathcal{D}_0$ the **bottom** of $\mathcal{M}_0$, and $\mathcal{D}_1$, $\mathcal{D}_2$ and $\mathcal{D}_3$ its **walls**, although the term of *bottom* has no real meaning in the $4D$ space. Our remark about the symmetry means that any other one of these dodecahedra could play the rôle of the bottom, the others being then the walls. As a consequence, the bottom will also be considered as a wall in many regards, as we shall see later.

Later on, we shall also call a wall the $3D$ space which is generated by some $\mathcal{D}_i$. By symmetry, we may consider that the numbering is in such a way that $\mathcal{D}_1$ is on the back of $\mathcal{D}_0$, and that $\mathcal{D}_1$ and $\mathcal{D}_2$ are on its shoulders, all these dodecahedra being obtained from $\mathcal{D}_0$ by the orthogonal completion. We can identify $\mathcal{D}_1$ with the dodecahedron Δ of the previous section. Then, by symmetry, $\mathcal{D}_0$ is on its back, and $\mathcal{D}_2$ and $\mathcal{D}_3$ are also on the shoulders of $\mathcal{D}_1$.

Now, $\mathcal{D}_1$, $\mathcal{D}_2$ and $\mathcal{D}_3$ share an edge, say $\mathbf{h}$, which is orthogonal to $\mathcal{D}_0$. The first hyper-corner which we delimit in $S_0 \setminus \mathcal{M}_0$ is the image of $\{\mathcal{D}_0, \mathcal{D}_1, \mathcal{D}_2, \mathcal{D}_3\}$ under the shift along $\mathbf{h}$ which transforms O into B, the other end of $\mathbf{h}$.

We shall now characterise $\mathbf{h}(\mathcal{M}_0)$, the image of $\mathcal{M}_0$ under this shift. Indeed, it will be enough to characterise the images of $\mathcal{D}_0$, $\mathcal{D}_1$, $\mathcal{D}_2$ and $\mathcal{D}_3$. To this purpose, we shall make use of the following lemma:

Fourth vector Lemma – *Consider five points O, M, N, P and Q such that OM, ON, OP and OQ are equal and pairwise perpendicular. Let Δ be the dodecahedron which is generated by three of these vectors, for instance by OM, ON and OP. Let F be a face of Δ which passes through O. We may assume that F is spanned by OM and ON. Then the dodecahedron which is constructed on F by the orthogonal completion with respect to Δ is spanned by the two vectors which span F, OM and ON, and by the fourth vector, OQ.*

The proof is straightforward from the definitions and it is left to the reader.

Under the shift $\mathbf{h}$, we see that the face DOF of $\mathcal{D}_1$, see the figure 14, is transformed into the face CBE. As in the plane DOB the image of OD is BC and, similarly, as in the plane FOB the image of OF is BE, we obtain that $\mathbf{h}(\mathcal{D}_0)$ is $\mathcal{D}_6$, the dodecahedron of the first generation which is obtained by the orthogonal completion on the face 6 of $\mathcal{D}_1$, with respect to $\mathcal{D}_1$. Notice that $\mathbf{h}(\mathcal{D}_1)$ is not represented in the figure: indeed, it is the reflection of $\mathcal{D}_1$ in $\mathcal{D}_6$ which is a hyper-face of $\mathcal{M}_0$.

Let us clarify this point. Let P denote the point of the line OB such that

B is the middle of OP. It is not difficult to see that $P = \mathbf{h}(B)$ and that P is the reflection of O in $\mathcal{D}_6$. Next, the plane DOB is globally invariant under the shift $\mathbf{h}$. The image of the plane DOB under the reflection in $\mathcal{D}_6$ is also the same plane: indeed, the plane is as well defined by OBC. Now, BC is invariant under the reflection and OB is transformed into PB which is on the same line as OB. These elements are enough to establish that $\mathbf{h}(\mathcal{D}_1)$ and the reflection of $\mathcal{D}_1$ in $\mathcal{D}_6$ are the same dodecahedron. We can view the representation of $\mathbf{h}(\mathcal{D}_1)$ as the representation of $\mathcal{D}_1$ itself, just imagining it as being put above $\mathcal{D}_1$ on the face CBE.

Accordingly, the two other dodecahedra of $\mathbf{h}(\mathcal{M}_0)$ are obtained by the orthogonal completion of the faces of $\mathcal{D}_6$ which are the images of the shoulders of $\mathcal{D}_0$ which are identified with the shoulders of $\mathcal{D}_1$. In the figure 14, see the small dodecahedra being developed on the sub-faces 1 and 5 of $\mathcal{D}_6$. We show them at a greater scale in the figure 15 where the big dodecahedron is $\mathcal{D}_6$.

Notice that the points P_1 and P_2 of the figure 15 correspond to identical points: they are two different views of P the image of O under the reflection in $\mathcal{D}_6$. Indeed, by the orthogonal completion being used to construct $\mathcal{D}_6$, BQ is perpendicular to BC, BE and OB. It is not difficult to see that $Q = \mathbf{h}(A)$, where A is represented by A_1 and A_2 in the figure 15. And so, $\{BQ, BC, BE, OB\}$ is an orthogonal basis of the space. As BC, BE and BQ span the hyper-plane being defined by $\mathcal{D}_6$, the orthogonal completion on the face being spanned by BC and BQ produces OB, by the Four Vector Lemma. Now, BQ is identified with the third edge of $\mathcal{D}_2$ which is on the shoulder DOB of $\mathcal{D}_1$ at the vertex B. And so, the dodecahedron which is built by orthogonal completion on the face 5 of $\mathcal{D}_6$ is in the hyper-plane being generated by $\mathcal{D}_2$. And so this dodecahedron is $\mathbf{h}(\mathcal{D}_2)$. This is not surprising: $\mathbf{h}$ belongs to this hyper-plane and so a shift of any figure being contained in the hyper-plane remains in this hyper-plane. By a similar argument, it is not difficult to see that the dodecahedron which is obtained by orthogonal completion on the other shoulder of $\mathcal{D}_6$ is $\mathbf{h}(\mathcal{D}_3)$.

At this point, we have already three dodecahedra which share the face CBE: $\mathcal{D}_1$, $\mathcal{D}_6$ and $\mathbf{h}(\mathcal{D}_1)$ which is the reflection of $\mathcal{D}_1$ in $\mathcal{D}_6$. From what we have seen in establishing the incidence table 1, it is clear that the fourth dodecahedron which shares BCE in $I\!H^4$ is the reflection of $\mathcal{D}_6$ in BCE.

Now, consider the face 5 of $\mathcal{D}_6$: it is the face in light pink in the figure 15. We know that by the orthogonal completion with respect to $\mathcal{D}_6$, the dodecahedron which we can build on this face is $\mathbf{h}(\mathcal{D}_2)$ which is in the same hyper-plane as $\mathcal{D}_2$. It is also the reflection of $\mathcal{D}_2$ in the face BCM of $\mathcal{D}_2$ in the figure 14: notice that the face BCM is identical to the face CBQ of $\mathcal{D}_6$.

This time, consider the dodecahedron $\mathcal{D}$ which is built on the face BCM by the orthogonal completion with respect to $\mathcal{D}_2$. By looking at the basis $\{BQ, BC, BE, OB\}$ which we considered above, and by reminding that OB and BP are on the same line, we see, by the Four Vector Lemma, that $\mathcal{D}$ is built on the vectors BC, BQ and BE, which spans $\mathcal{D}_6$. Accordingly, the four dodecahedra which share the face BCM in $I\!H^4$ are $\mathcal{D}_6$, $\mathcal{D}_2$ and their reflections in their common face BCM. This face is the intersection of two perpendicular hyper-planes: one is defined by $\mathcal{D}_6$, the other one by $\mathcal{D}_2$.

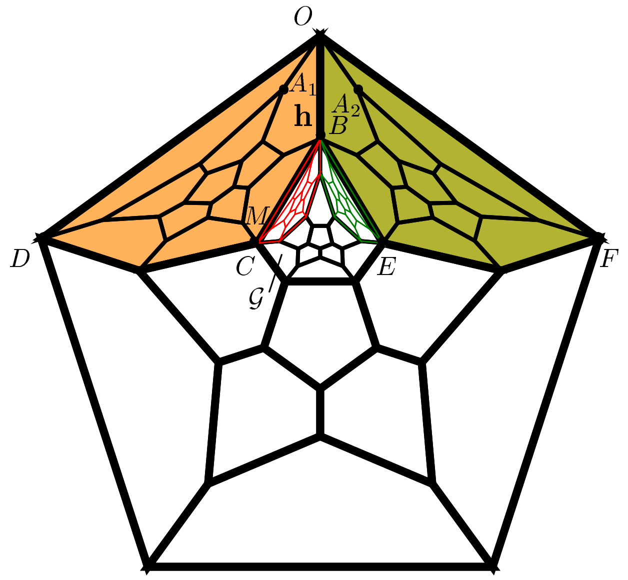

Figure 14. The shift of the basic hyper-corner

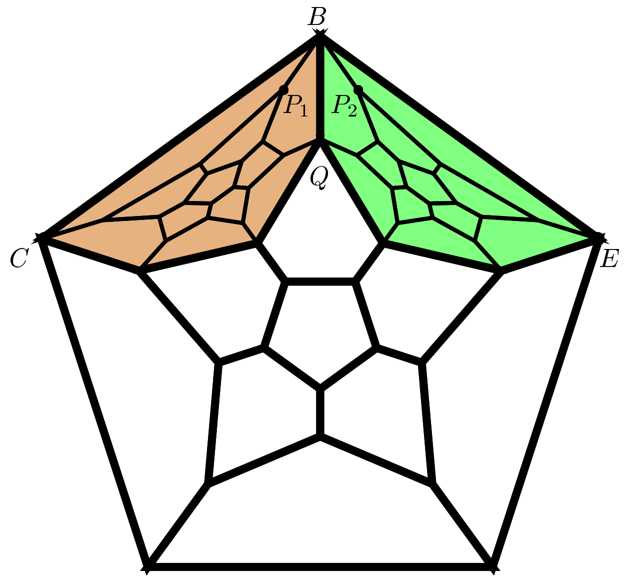

Figure 15. The image shift of the basic hyper-corner in the face 6 of the basic dodecahedron

Now, we know that $\mathcal{D}_2$ is a wall for $\mathcal{M}_0$. And so, its reflection in BCM is still in the same hyper-plane and so it is the continuation of the previous wall to $\mathbf{h}(\mathcal{M}_0)$. This is the reason why the face 5 of $\mathcal{D}_6$ is shadowed in the figure 15. For a similar reason, we also shadowed the face 1 of $\mathcal{D}_6$.

In order to complete the description of the situation, we can see that the reflection of $\mathcal{D}_6$ in BCM is outside $\mathcal{M}_0$. where it would be the common hyper-face of two 120-cell which are outside $\mathcal{M}_0$ and which lean on the wall being defined by the hyper-plane of $\mathcal{D}_1$.

We have now a last remark. The four dodecahedra which we identified in the definition of $\mathbf{h}(\mathcal{M}_0)$ define a 120-cell $\mathcal{M}_1$ which is the reflection in $\mathcal{D}_6$ of the original 120-cell $\mathcal{M}_0$ being constructed on $\mathcal{D}_0$, $\mathcal{D}_1$, $\mathcal{D}_2$ and $\mathcal{D}_3$. Indeed, we saw that $\mathbf{h}(\mathcal{D}_1)$ is the reflection of $(\mathcal{D}_1)$ in $\mathcal{D}_6$ and that $\mathbf{h}(\mathcal{D}_2)$ is the reflection of $\mathcal{D}_2$ in BCM. But the face BCM is the face BCQ of $\mathcal{D}_6$, and so the reflection of $\mathcal{D}_2$ in BCM is also the reflection of $\mathcal{D}_2$ in $\mathcal{D}_6$. Similarly, we get that $\mathbf{h}(\mathcal{D}_3)$ is the reflection of $\mathcal{D}_3$ in $\mathcal{D}_6$. As a 120-cell is characterised by four of its hyper-faces which share a common vertex, we get that $\mathcal{M}_1$ is the reflection of $\mathcal{M}_0$ in $\mathcal{D}_6$.

All these considerations prove the following lemma which will be repeatedly used further:

Hyper-corner Lemma – *Let four dodecahedra $\mathcal{D}_0$, $\mathcal{D}_1$, $\mathcal{D}_2$ and $\mathcal{D}_3$ share a common vertex O and be pairwise perpendicular, sharing pairwise a common face. Consider another vertex B, sharing an edge of these dodecahedra with O. Consider the three dodecahedra sharing OB, for instance, $\mathcal{D}_1$, $\mathcal{D}_2$ and $\mathcal{D}_3$. Consider one of these dodecahedra, say $\mathcal{D}_1$. Let F and G be the two faces of $\mathcal{D}_1$ sharing OB. Then the image under the shift along OB of the 120-cell $\mathcal{M}$ being constructed on $\mathcal{D}_0$, $\mathcal{D}_1$, $\mathcal{D}_2$ and $\mathcal{D}_3$ is the reflection of $\mathcal{M}$ in the image of $\mathcal{D}_0$ under the same shift. In particular, we have that the image of $\mathcal{D}_1$ under the shift is its reflection in H, where H is the third face of the dodecahedron $\mathcal{D}_1$ which contains B. As a consequence, this reflection is in the same hyper-plane as $\mathcal{D}_1$.*

Now, consider the face $\mathcal{G}$ of $\mathcal{D}_6$ which is indicated in the figure 14. It is easy to see that $\mathcal{M}_0$ is also generated by $\mathcal{D}_1$, $\mathcal{D}_2$, $\mathcal{D}_3$ and $\mathcal{D}_6$, where $\mathcal{D}_3$ plays the rôle which was formerly the rôle of $\mathcal{D}_0$, and where $\mathcal{D}_6$ plays the same rôle as $\mathcal{D}_3$ formerly. From the Hyper-corner Lemma, the reflection of $\mathcal{M}_0$ in the dodecahedron which is constructed on the face 10 of $\mathcal{D}_1$ by orthogonal completion, say $\mathcal{D}_{10}$ is the image of $\mathcal{M}_0$ under the shift along BC. Call $\mathcal{M}_2$ this new 120-cell. From our previous study, and from the Hyper-corner Lemma, the four dodecahedra which share the face $\mathcal{G}$ of the figure 14 are $\mathcal{D}_1$, $\mathcal{D}_6$, the reflection of $\mathcal{D}_6$ in $\mathcal{G}$, hence in $\mathcal{D}_{10}$, and the reflection of $\mathcal{D}_{10}$ in $\mathcal{G}$. As $\mathcal{D}_2$ is a wall for $\mathcal{M}_0$, it is also a wall for $\mathcal{M}_2$.

We know already three 120-cell which also share $\mathcal{G}$: $\mathcal{M}_0$, $\mathcal{M}_1$ and $\mathcal{M}_2$. Let $\mathcal{M}_1'$ be the reflection of $\mathcal{M}_1$ in the image of the reflection of $\mathcal{D}_{10}$ in $\mathcal{G}$, and let $\mathcal{M}_2'$ be the reflection of $\mathcal{M}_2$ in the image of the reflection of $\mathcal{D}_6$ in $\mathcal{G}$. $\mathcal{M}_1'$ shares a dodecahedron with $\mathcal{M}_1$: the reflection of $\mathcal{D}_{10}$ in $\mathcal{G}$. Accordingly, $\mathcal{M}_1'$ contains $\mathcal{G}$. Similarly, as the reflection of $\mathcal{D}_6$ in $\mathcal{G}$ contains also $\mathcal{G}$, $\mathcal{M}_2'$

contains also $\mathcal{G}$. And so, we obtain two 120-cell which are different from the previous ones and which also share $\mathcal{G}$. Accordingly, from the indication of the incidence table 1, these two 120-cells coincide and they constitute the fourth 120-cell which contains $\mathcal{G}$.

And so, as these two reflections produce the same 120-cell, we have to forbid one of them and to promote the other one. Notice that we constructed $\mathcal{M}_1$ first and then $\mathcal{M}_2$. Notice also that $\mathcal{G}$ is contained by $\mathcal{D}_6$ and by the reflection of $\mathcal{D}_6$ in $\mathcal{G}$ and that both these dodecahedra are in the same hyper-plane. Accordingly, it is natural to consider that the hyper-plane being generated by $\mathcal{D}_6$ is a wall for $\mathcal{M}_2$: this is a possible interpretation of the above shift $\mathbf{k}$ which transports the situation of $\mathbf{h}(\mathcal{M}_0)$ to $\mathcal{M}_2$. And so, we forbid the reflection of $\mathcal{M}_2$ in that hyper-plane and we promote the reflection of $\mathcal{M}_1$ in the hyper-plane being generated by $\mathcal{D}_{10}$ which is the hyper-plane of the dodecahedron which is constructed on $\mathcal{G}$ by the orthogonal completion with respect to $\mathcal{D}_6$.

We indicate this choice by shadowing the image of $\mathcal{G}$ which lies in the representation of $\mathcal{D}_{10}$ as it is indicated in the figure 16. This is a shadowing which looks like to the one which the author introduced in [14], but which is not obtained in the same way. Indeed, here, we shadow one image of the same face and not the other image in order to indicate on which side the reflection is forbidden: in this way, we take advantage of the fact that the same face has two representations in the Schlegel diagram.

And so, here, we have two reasons for shadowing a face: to continue a wall, and to start a wall. The continuation of a wall explains the shadowing of the face 5 of $\mathcal{D}_6$ the orthogonal complement of which continues the wall of the wall which is defined by $\mathcal{D}_2$, the orthogonal complement of the face 5 of $\mathcal{D}_1$. Starting a new wall is illustrated by the just performed discussion about the face $\mathcal{G}$. At this point, recall that the bottom is also a wall in this regard. This induces two simple rules:

Shadowing Rules:

- *If a face of a new generation is adjacent to a shadowed face of the previous generation, it must be shadowed.*
- *When two identified faces appear at the same generation, one of them must be shadowed and the other one must remain un-shadowed.*

In these rules, generations are understood in the meaning given to this word during the construction of the 120-cell.

The starting point in the application of these rules is that the walls and the bottom of the initial 120-cell are considered as shadowed.

Before going on with the splitting process, we conclude this sub-section with a remark on the **analogy** of situation between the $4D$ case and the $3D$- and $2D$- cases.

The first analogy lies in the dimensional shift which we can observe from the incidence tables. We produce them here in the table 13 for the dimensions 2, 3 and 4, replicating again the table 1. The reader can establish then very easily by applying the method which we used for the table 1.

And so, we see that the rôle of the vertices in the plane is played by the edges in $\mathbb{H}^3$ and by the faces in $\mathbb{H}^4$. In the same way, the rôle of the edges is played by the faces in $\mathbb{H}^3$ and by the dodecahedra in $\mathbb{H}^4$. The same observation holds, respectively, for the pentagon, the dodecahedron and the 120-cell.

	0	1
1	4	
2	4	2

	0	1	2
1	6		
2	12	4	
3	8	4	2

	0	1	2	3
1	8			
2	12	6		
3	32	12	4	
4	16	8	4	2

	0
1	2

	0	1
1	3	
2	3	2

	0	1	2
1	4		
2	6	3	
3	4	3	2

Table 13. The tables of incidence in $\mathbb{H}^2$, $\mathbb{H}^3$ and $\mathbb{H}^4$ and then in the pentagon, the dodecahedron and the 120-cell.

Another analogy can be observed in the elements of S_0. In the plane, S_0 is a quarter, *i.e.* a 4^{th} of the space. In $\mathbb{H}^3$, it is an octant, *i.e.* an 8^{th} of the space, and in $\mathbb{H}^4$, it is a hyper-corner, *i.e.* an 16^{th} of the space. In the plane, the walls of S_0 are lines. In $\mathbb{H}^3$, they are planes and in $\mathbb{H}^4$, they are hyper-planes.

In the splitting, in $\mathbb{H}^2$, the first shift is performed along an edge which connects the vertices of the initial quarter and its image. This is the case also in $\mathbb{H}^3$ and in $\mathbb{H}^4$. In $\mathbb{H}^2$, the original quarter shares a line with its image, and the other line of the quarter is non-secant with its image. Moreover, the common line is the common perpendicular between that line and its image. In $\mathbb{H}^3$, the original octant shares two planes with its image and the third plane is non-secant with its image. Moreover, the line of the shift is the common perpendicular between the third plane and its image. In $\mathbb{H}^4$, the original hyper-corner shares three hyper-planes with its image: $\mathcal{D}_1$, $\mathcal{D}_2$ and $\mathcal{D}_3$. The fourth hyper-plane, $\mathcal{D}_0$ is non-secant with its image $\mathcal{D}_6$. The line of the shift is the common perpendicular of $\mathcal{D}_0$ and $\mathcal{D}_6$.

These analogies are one of the most convincing arguments of the correctness of the construction. They will be a useful guide for the continuation of the process.

5.2 The geometrical part of the splitting

We can now proceed to the continuation of the splitting. First, we shall deal with the faces of the first generation, then with the second and so on, generation after generation, until we arrive to the single dodecahedron of the eighth generation.

When this process will be completed, we shall then turn to the algebraic side of the splitting.

5.2.1 The first generation

Now, we are ready to go on the process to the other faces of $\mathcal{D}_1$ which are used during the construction of the dodecahedra of the first generation.

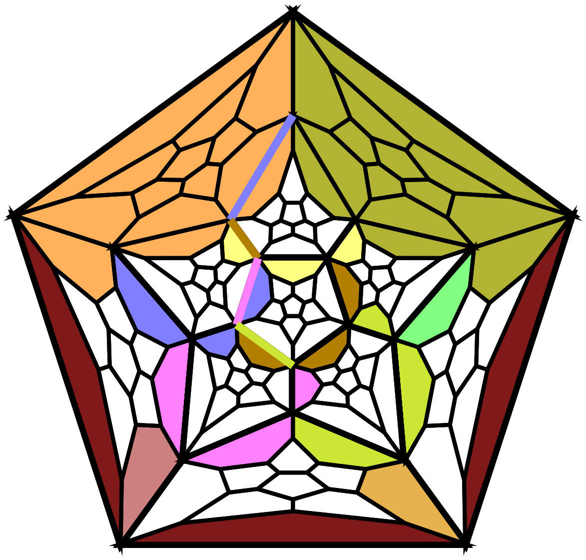

Figure 16. Splitting the basic hyper-corner: first generation Notice the various shifts being indicated by a coloured broken line.

We already noticed that the progression on the faces of $\mathcal{D}_1$ is very similar to what was done in the $3D$ case in [14]. Notice that this gives us five hyper-corners. When we arrive to the face 7 of $\mathcal{D}_1$,see the figure 16, the dodecahedron which is built there by the orthogonal completion with respect to $\mathcal{D}_1$ is already limited by two walls: one is the continuation of $\mathcal{D}_3$ and the other is produced by the construction of $\mathcal{D}_8$ which is processed just before $\mathcal{D}_7$. And so, we arrive to a region which is grounded on $\mathcal{D}_1$ with four walls around the face 7 of $\mathcal{D}_1$. Next, we meet two other regions of this type, which are constructed on the face 2 and then on the face 3. When we arrive on the face 4, we meet an additional wall due to the fact that we fall again on $\mathcal{D}_2$.

Indeed, we have a new region which is $\mathcal{D}_1$ being surrounded by five walls.

It is possible to sum up this information by the table 14, below.

We shall also symbolise the unbounded elements of the basis of splitting which we determined at this stage of the process by the pictures which are displayed by the figure 17.

We notice that we have here 3 kinds of regions: in the first one, the ground has two walls, in the second one, it has four walls, and in the third one, it has five walls. We shall name this regions after the number of their faces which are not covered by a wall. For the regions which we already defined, we obtain, respectively: 9, 7 and 6 faces.

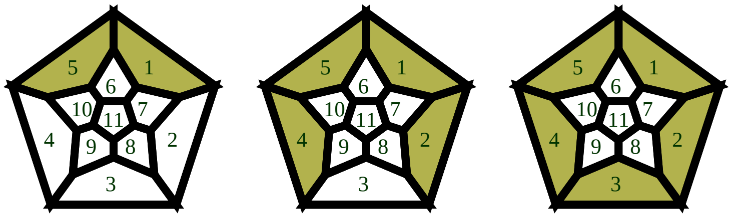

Figure 17. The regions of the first generation

	9	8	7	6
I	5	0	3	1

Table 14. The matrix of the splitting: beginning of the counting process.

5.2.2 The second and the third generations

Now, consider the situation for the second and for the third generations.

Construction of the basic polyhedron by generations

The first point which we have to consider is how the splitting goes from the first generation to the second one. We remember that during the process of the construction of the 120-cell, at the beginning of a new generation, the usual expression was "let us put a dodecahedron on such and such faces". This expression was a simple synonym to say that we perform the orthogonal completion of the basic dodecahedron on the considered face.

Consider the second generation. In this way we put a dodecahedron on each face of the inner ring of the dodecahedra of the first generation. As an example, we put a dodecahedron on the face 6 of $\mathcal{D}_6$. This does not mean that the new dodecahedron appears in the hyper-corner $\mathcal{M}_1$ which we defined in the previous sub-section. The new dodecahedra appear outside this hyper-corner.

Let us look again at the process in the plane and in $I\!H^3$. In these contexts, the situations are much more simple and we do not need to use several generations in order to construct, respectively, a pentagon and a dodecahedron.

However, we can view the process of construction a pentagon as consisting of two generations. Initially, we have a segment E of the required length. The first generation consist in putting a new segment at the ends of E, perpendicularly to E and in the same half-plane with respect to E: this is exactly the orthogonal completion of E on each of its faces. This first generation consists of two segments, E_1 and E_2 and each of them has a free end which can be orthogonally completed with respect to its segment. This is the second generation which also consists in two segments, E_3 and E_4. As the segments are equal and as they have the required length, the new ends of E_3 and E_4 meet and this completes the construction of the pentagon.

In the case of the plane, the splitting process starts with the definition of the initial quarter which we can define by E and one of the segments of the first generation, say E_2. And so, the first new quarter of the splitting $\mathcal{Q}_1$ is defined by the shift along E which transforms E_2 into E_1, and we see that the whole second generation lies outside $\mathcal{Q}_1$.

In the case of the dodecahedron in $I\!H^3$, the process is the same. We start with a pentagon P and we complete each one of its side by a new pentagon which is orthogonal to P and shares with it the considered side in such a way that all the new pentagons, P_1 up to P_5 are in the same half-plane being delimited by P. The P_i's constitute the first generation. At this stage, each P_i shares two sides with two of the other P_j's and so, each one has two free sides. We complete them orthogonally by new pentagons. A priori we need ten pentagons but two neighbouring free edges belonging to different P_i's yield the same pentagon of the second generation, and so we have five pentagons, P_6, ..., P_{10} for the second generation. By construction, each P_i of the second generation shares two edges with the first generation and two edges with its neighbours of the same generation. Consequently, each has only a single free edge. The orthogonal completion of the pentagons of the second generation on their free edge produces the same pentagon, P_{11}, which completes the construction. Notice that this corresponds to the numbering which we introduced at the beginning.

In this case, the splitting has the same property as in $I\!H^2$. The initial octant, $\mathcal{Q}$, is defined by P and two adjacent pentagons of the first generation, for instance P_1 and P_5: see the bold numbers in the figure 18, P_i being numbered by **i**. The first new octant of the splitting is obtained analogously by the shift in the plane being defined by P_1 which transforms P_5 into P_4. The octant which is built on this place leaves all the other faces outside it. We observe the same property for the next octant which uses the continuation of the plane being generated by P_4 and the plane being generated by P_3. Next, when we arrive at P_2, we have both the plane of P_3 and the plane of P_1 as walls. This produces a new type of region which I call a half-octant, see [14]. On this example, it is plain that in the splitting which is performed first on the elements of the same generation, the regions which are defined step by step leave outside them the elements which were not yet used at the considered stage.

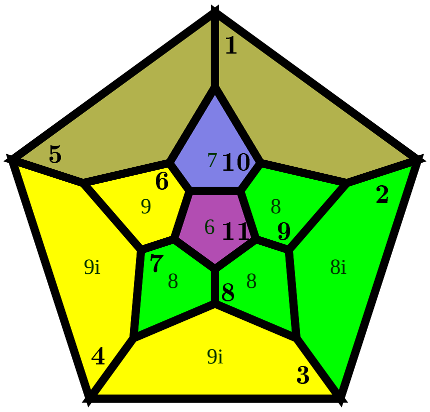

Figure 18. Splitting the octant in $I\!H^3$, generation after generation. The first generation is indicated by i, the second corresponds to the inner ring and the third generation contains a single element: the top of the initial dodecahedron. In bold symbols, we give the numbers of the faces.

We notice here that the splitting which is induced by the process being just described and illustrated in the figure 18 gives the same polynomial as the one which is indicated in [15]. We go back to that point in the next section where we deal with the algebraic aspects of the splitting.

Interior and exterior: a new visit

The new visit which we paid to $I\!H^2$ and $I\!H^3$ shows us that proceeding generation after generation is a correct way to obtain the expected splitting.

We shall see now that the elements of the further generations are outside the regions which we defined up to now.

For this purpose, we go back to the definition of the interior and the exterior of a hyper-face the 120-cell which we defined in the sub-section 3.3.

We repeat that the views are totally misleading in that regard because they do not give an account of the possibility to move around a plane in the $4D$ space.

Here we extend the notion of the interior of a hyper-face of the 120-cell to hyper-corners and, more generally, to the regions which will be involved in the construction of the splitting. As a hyper-corner is defined by four pairwise perpendicular dodecahedra, by definition, its **interior** is the intersection of the half-spaces being determined by the dodecahedra which contain all four dodecahedra or the half-spaces which meet all four dodecahedra. We give this precision, due to the *abus de langage* which was introduced in the sub-section 3.3: the interior can be understood as an open domain or as including also the border of that domain. It will be clear from the context what is the exact meaning.

This can be easily generalised to any region being defined as the intersection of hyper-planes being defined by a sequence of adjacent hyper-faces of a common 120-cell.

It is easy to see that the reflection in a hyper-face F of a 120-cell exchanges its interior and exterior sides. Consequently, the reflection of a hyper-face $\mathcal{D}_j$ in the hyper-face $\mathcal{D}_i$ lies in the exterior of $\mathcal{D}_i$, we shall say **outside** $\mathcal{D}_i$.

Consider now the first hyper-corner being constructed in the process, $\mathcal{M}_1$. We know that $\mathcal{M}_1$ is defined by $\mathcal{D}_6$, the reflection of $\mathcal{D}_2$ in $\mathcal{D}_6$, the reflection of $\mathcal{D}_3$ in $\mathcal{D}_6$ and the reflection of $\mathcal{D}_1$ in $\mathcal{D}_6$. As the interior of the hyper-corner must contain all just considered dodecahedra, from the previous remark about the exterior of a hyper-face, in order to be outside $\mathcal{M}_1$, it is enough to be in the exterior of at least one hyper-face of the 120-cell being different from $\mathcal{D}_6$.

And so, we see that what we observed in $I\!H^2$ and in $I\!H^3$ also holds in $I\!H^4$. Notice also another analogy: from our study of the first generation, we notice that each $\mathcal{M}_i$ for $i \in \{1..9\}$, have the hyper-plane being generated by $\mathcal{D}_1$ as one of their walls. In a similar way, for all the regions of $I\!H^2$ which belong to the first generation, the bottom is in the same plane as the bottom of the initial octant. Also in $I\!H^2$, the first quadrant is delimited by the line which supports the initial segment.

As a last remark, notice that this definition sheds a new light onto the shadowing process: indeed the shadowing guarantees that the splitting is allowed only in the bf interior of the regions which are defined.

The splitting in the second generation

We have now all the tools in order to proceed to the second generation.

Our first task consists in indicating the walls which derived from the already determined regions. At this stage, notice that the walls appear on the outer faces of a dodecahedron. Such faces appear by pairs around the outer edges: one in a dodecahedron, the other one, in the other dodecahedron which shares the edge. The figure 19 illustrates this situation. In order to have a readable figure, we did not shadow the faces in the outer ring of the dodecahedra of the first generation. We just indicate the walls which are inherited from the first splitting which is illustrated by the figure 16. This shadowing is obtained by a simple application of the Shadowing Rules. Notice that, here, both rules apply. Notice, in particular, that we have the continuation of the wall being defined by $\mathcal{D}_0$ in the neighbouring sub-faces in all the outer faces of $\mathcal{D}_1$.

In the figure, we number the vertices from 10 until 29, as there are twenty of them, as we know, and we start from the shoulders of $\mathcal{D}_1$ and then, we proceed on its faces level by level, from left to right. From the study of the elements of the second generation, we also remember that if we develop Schlegel diagrams on each cell of the first generation which can receive a new dodecahedron, we do not obtain sixty new dodecahedra but only twenty ones. There are sixty dodecahedra in the figure because each true dodecahedron of the second generation is represented by three dodecahedra which are displayed symmetrically around a vertex and which represent three views of the true dodecahedron. The numbering of the vertices allows us to locate the new dodecahedra. Notice that we see exactly fifty five dodecahedra on the figures 19 and 20: the missing five ones belong to the back of $\mathcal{D}_1$ which is not seen in the figures.

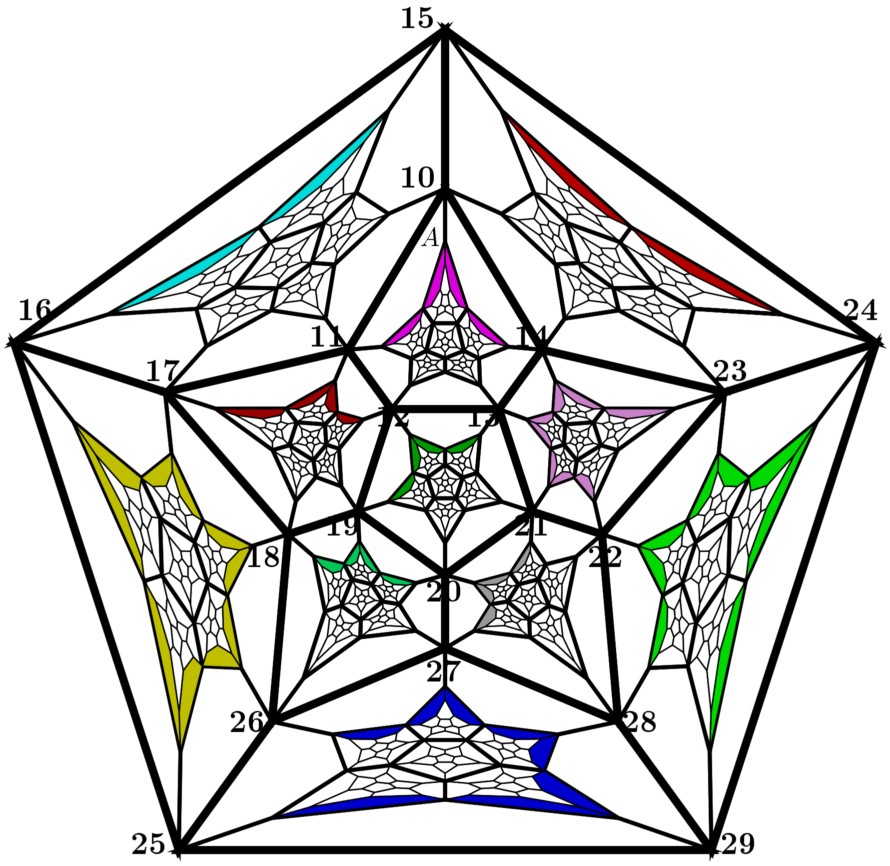

Figure 19. Splitting the basic hyper-corner: the walls being inherited from the first generation

For this generation, we shall denote the dodecahedra by $\mathcal{E}_i$, where i is the number of the vertex around which the three views of $\mathcal{E}_i$ are displayed.

For the first hyper-corner, we take the face 6 of $\mathcal{D}_6$ as a basis of our construction, and we consider as $\mathcal{E}_{10}$ the dodecahedron which is obtained on this face by the orthogonal completion with respect to $\mathcal{D}_6$. It is not difficult to notice that $\mathcal{E}_{10}$ is obtained as the image of $\mathcal{D}_6$ by the shift which transforms the vertex 10 into the point A of the figures 19 and 20.

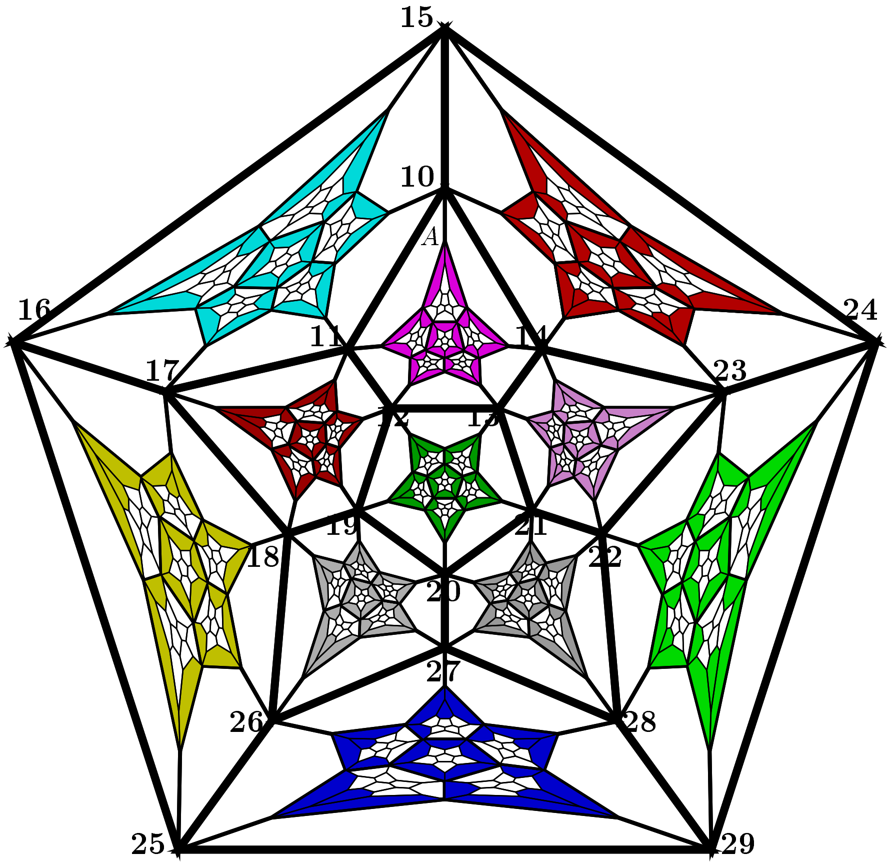

Figure 20. Splitting the basic hyper-corner: second and third generation

From the walls being established at the first generation, the faces 1 and 5 of $\mathcal{E}_{10}$ are shadowed: they indicate the continuation of the walls being defined by $\mathcal{D}_2$ and $\mathcal{D}_3$. There is no other constraint for this dodecahedron and so, we can fix here a hyper-corner. As we first consider the face 1 of $\mathcal{D}_6$, we see on the views of the dodecahedra $\mathcal{E}_{10}$ up to $\mathcal{E}_{14}$, it seems that the faces of these dodecahedra which play the rôle of the shadowed faces of $\mathcal{E}_{10}$ are not shadowed. This is not the case. If we consider $\mathcal{E}_{11}$ for instance, the shadowing of those faces appear on the views of that dodecahedra which belongs to the face 6 and to the face 10 of $\mathcal{D}_1$. And so, as $\mathcal{E}_{10}$ itself induces a shadowing on the adjacent outer faces of the adjacent $\mathcal{E}_i$'s, we see that on $\mathcal{E}_{11}$, three faces have to be shadowed. In order to make the correspondence with the identical faces of different views, we make use of the figure 5.

As an illustration, we may observe that, for instance, the three views of $\mathcal{E}_{11}$ are not similar: two of them are 'symmetric', the views of the faces 1 and 6, but the view of the face 10 is not. In this view the sides of $\mathcal{E}_{11}$ are free, as long as $\mathcal{E}_{11}$ is the first dodecahedron being constructed on $\mathcal{D}_{10}$. But the third view has also three shadowed face: the shadowed sides of the other views correspond to the head of this one. Notice also that the view of $\mathcal{E}_{11}$ was already shadowed in the figure 19. The other shoulder must also be shadowed: it is a view of the back of the view of $\mathcal{E}_{11}$ which lies on the face 10. As this face is in contact with $\mathcal{D}_{10}$ which is the bottom of $\mathcal{E}_{11}$ in this view, the considered shoulder has also to be shadowed.

Proceeding step by step in this way, and especially taking into account the information being provided us by the figure 5, we obtain the shadowing which is indicated by the figure 20.

Let us indicate some features of this process.

When we proceed in the face 6 of $\mathcal{D}_6$, we notice that $\mathcal{E}_{11}$ does not define a nine-faced region as $\mathcal{E}_{10}$, but only an eight-faced region: one wall is produced by the wall of $\mathcal{D}_2$, another one is produced by the view of a wall in the other view of $\mathcal{E}_{11}$ and the third one is produced by the wall being generated by $\mathcal{E}_{10}$. Using the correspondence between three views which is given by the figure 5, we arrive to the following three kinds of regions:

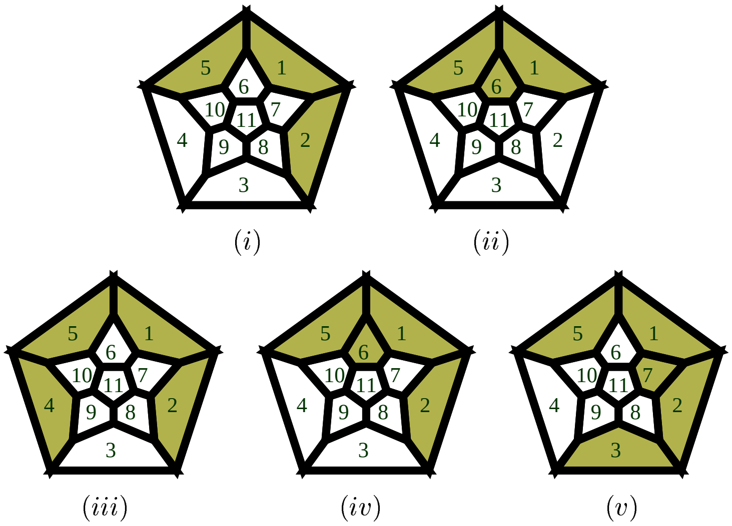

Figure 21. Regions of the second generation

Notice that the numbering on the region which is displayed in the middle of the figure corresponds to the faces with the same number in the left hand region. This shows that the two regions are the same: we obtain them by rotating the dodecahedron on another face. In the picture of the middle part of the figure, the back is the face 2. But we obtain also a new region which is produced by $\mathcal{E}_{29}$ and which is illustrated by the figure 21.(iii). As it can be deduced by the above argument and as it is shown in the figure 20, this new region is also a six-faced one. But this region is different from the six-faced region which is illustrated in the figure 17. In the case of the figure 17, there is a shadowed face which is surrounded by shadowed faces only. This is not the case for the figure 21.(iii): all its shadowed faces have at least one neighbour which is white.

From now on, we shall denote the six-faced region of the figure 17 as $6a$ and the six-faced region of the figure 21 as $6b$.

The figure 20 indicates us also the kind of region which corresponds to each dodecahedron of the third generation. It is a six-faced region which is analogous to the right hand picture of the figure 17.

The table 15 gives us the counting of the different kind of regions. The table indicates the number of **free** faces of the dodecahedra, *i.e.* of the faces for which the reflection in the orthogonal completion being constructed on the face is promoted. This number consists in subtracted from the total number of faces, the shadowed faces and the back: indeed, the back of the dodecahedra are in contact with the dodecahedra of the previous generation. Recall that they are walls for the present generation: a reflection in them would produce objects lying inside the 120-cell.

	9	8	7	$6a$	$6b$
II	1	9	9	0	1
III	0	0	0	12	0

Table 15. The matrix of the splitting: counting the contribution of the second and of the third generations.

Before turning to the fourth generation, we notice that the considerations which we developed about the interior and exterior of the hyper-faces being involved in our constructions allow us to see that at each step, the hyper-faces which are not yet processed are **outside** the regions which are previously defined.

5.2.2 The fourth and the fifth generation

Now, we proceed with the fourth generation. We use the information which we obtained in the sub-section 4.6.

From this information, especially the figures 7 and 8, and the information of the sub-section 4.7. for the fifth generation, we know that any dodecahedron of the fourth generation has at least three shadowed faces and so it has at most eight free faces. As we already noticed, the back of the dodecahedron is always as a shadowed face: the dodecahedron of the third generation to which the face also belongs is a wall for the fourth generation. In the same way, the shoulders of the dodecahedra of the fourth generation are shadowed by the walls being established by the third generation. Their head is also shadowed: on the other view of the dodecahedron, it is its back.

For the shadowing, we proceed exactly as for the second and the third generation. We take the information of the sub-sections 4.6 and 4.7. We also use the same convention as in the figures 19 and 20. We consider that the twelve dodecahedra of the third generation are denoted by $\mathcal{E}_i$ with $i \in \{30..41\}$.

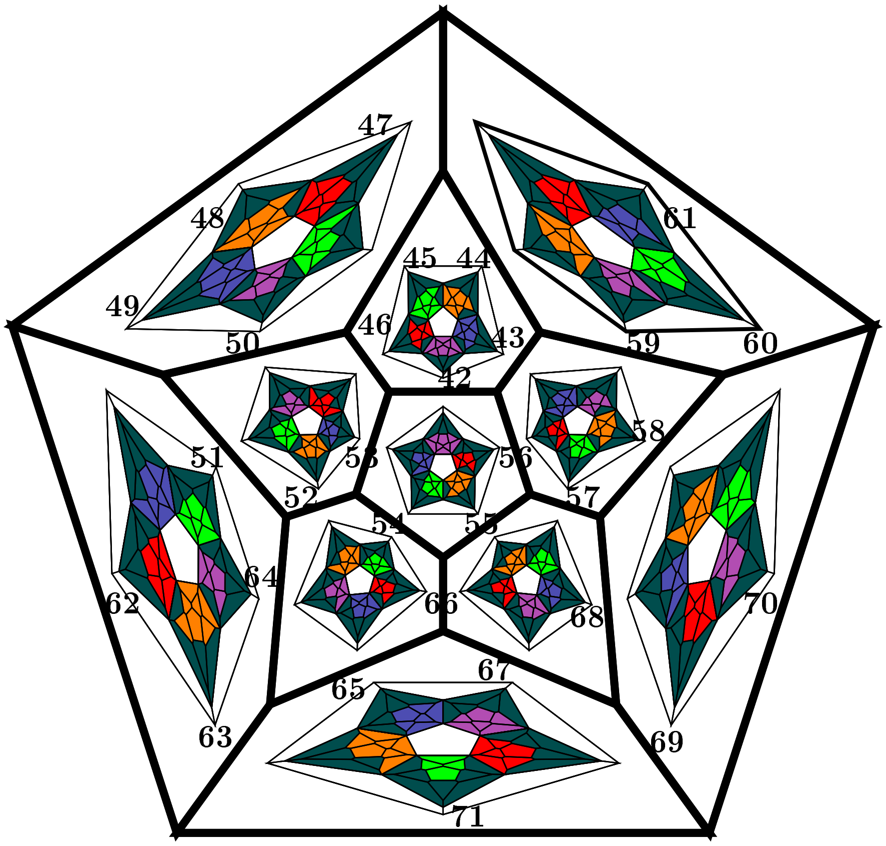

Figure 22. Splitting the basic hyper-corner: the walls for the fourth generation

Next, the dodecahedra of the fourth generation will be denoted by $\mathcal{E}_i$, with $i \in \{42..71\}$. We start with $\mathcal{E}_{42}$ which has two views: one in the face 6 of $\mathcal{D}_1$, and the other one in the face 10 of $\mathcal{D}_1$. For the numbering, we observe the same way as for the second generation. As we can see in the table 16, the splitting being proceeded in this order produces a symmetric table, as this was the case for the second generation. Later, in the section 6 which is devoted to the algebraic side of the splitting method, we shall examine the possibility of other splittings.

Notice that the fifth generation is exactly as the third one, being constituted of regions of the type $6.a$.

	8	7	$6a$	$6b$	5	4
IV	1	9	9	1	9	1
V	0	0	12	0	0	0

Table 16. The matrix of the splitting: counting the contribution of the fourth and of the fifth generations.

A close examination of the figure 22 shows us that the splitting process defines six kinds of regions for the fourth generation. The figure 23 illustrates the regions which appear at the present stage of the splitting, besides the kinds of regions which were already registered at the second generation.

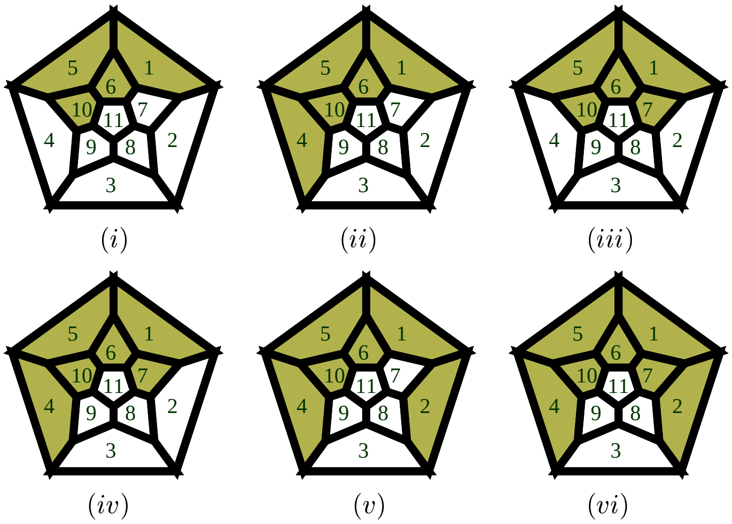

Figure 23. Regions of the fourth generation

Notice that some of the regions which appear during the splitting of the fourth generation already appear during the second generation. This is the case of the single region with eight face, being associated with $\mathcal{E}_{42}$ which is illustrated by the figure 21.(ii). It is also the case of regions with seven faces, another view of which was given by the figure 21.(iv) see, for instance, the region being associated with $\mathcal{E}_{43}$. The figure 22 shows a new view of such a region which is displayed by the figure 23.(i). The single region of the type $6.b$ which is associated with $\mathcal{E}_{46}$ has two views in the figure 22. One of them was already given in the figure 21.(v), and the second one appears in the figure 23.(iii). The figure 22 provides us with new views of the regions of the type $6.a$. We see them in the figure 23.(ii). The new regions, being introduced by the fourth generation, are the regions with five faces, as for instance, the region being associated to $\mathcal{E}_{53}$. The two possible views of this type of regions are given by the figure 23.(iv) and (v). There is a single region with four faces, being associated with $\mathcal{E}_{71}$. It is illustrated by the figure 23.(vi).

5.2.3 The sixth and the seventh generation

The splitting in the sixth generation

We proceed now to the sixth generation. The figure 24 illustrates the splitting at the stage of the sixth generation.

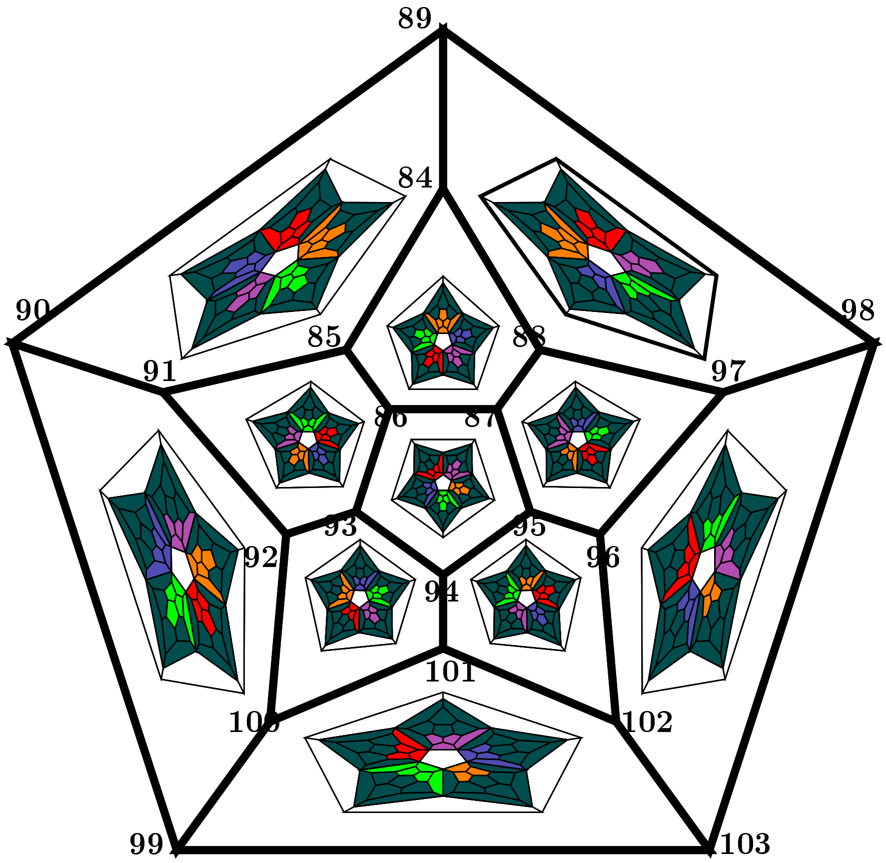

Figure 24. Splitting the basic hyper-corner: the walls being defined by the sixth generation

The dodecahedra of the fifth generation are numbered from $\mathcal{E}_{72}$ up to $\mathcal{E}_{83}$. Accordingly, the dodecahedra of the sixth generation are numbered from $\mathcal{E}_{84}$ up to $\mathcal{E}_{103}$.

The previous principles are also in action here. We see that the first region which is produced by the splitting has at most six faces, see the views of $\mathcal{E}_{84}$ in the figure 24. This information is a consequence of our study in the sub-section 4.8. Notice that the three views of the dodecahedron are identical: this is due to the symmetry of the situation and of the figure 23.(iii). For the other regions, we use the information of that sub-section, in particular the correspondence between the views which is provided us by the figure 11. The numbering which is given on the partial figures is intensively used in the figure 24.

The figure 25 sums up the new views of the regions which appear in the figure 24. This is the case, for instance, of the five-faced regions, as the region being attached to $\mathcal{E}_{85}$. We know already the views being displayed by the figures 23.(iv) and 23.(v). A new view appears in the figure 25.(i). We also know the view of the figure 23.(vi) for the four-faced region of the fourth generation. Here, the region being associated with $\mathcal{E}_{88}$ shows two new views, which are indeed symmetric images of one another. This new view is displayed by the figure 25.(ii). At last, there is a single region with three faces: it is associated with the dodecahedron $\mathcal{E}_{103}$. We have only two views of it which are symmetric and which are given by the figure 25.(iii).

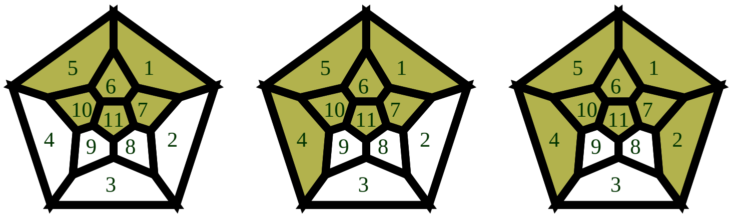

(i) (ii) (iii)

Figure 25. The new regions of the sixth generation.

The splitting in the seventh generation

At first glance, it seems surprising that the situation of the seventh generation is not at all the same as the situation in the third and in the fifth ones.

In fact, there is some symmetry in the generations which appear during the construction of the 120-cell and, accordingly, the seventh generation has some analogy with the first one. And we saw for the latter generation, that the dodecahedra of this generation do not play the same rôle.

We use the sub-section 4.9 and, especially, the information of the figure 13. From the latter figure, we know that the dodecahedra of the seventh generation have the same kind of neighbourhood as those of the first generation. And so, defining a region for one of them induces walls on the neighbouring ones.

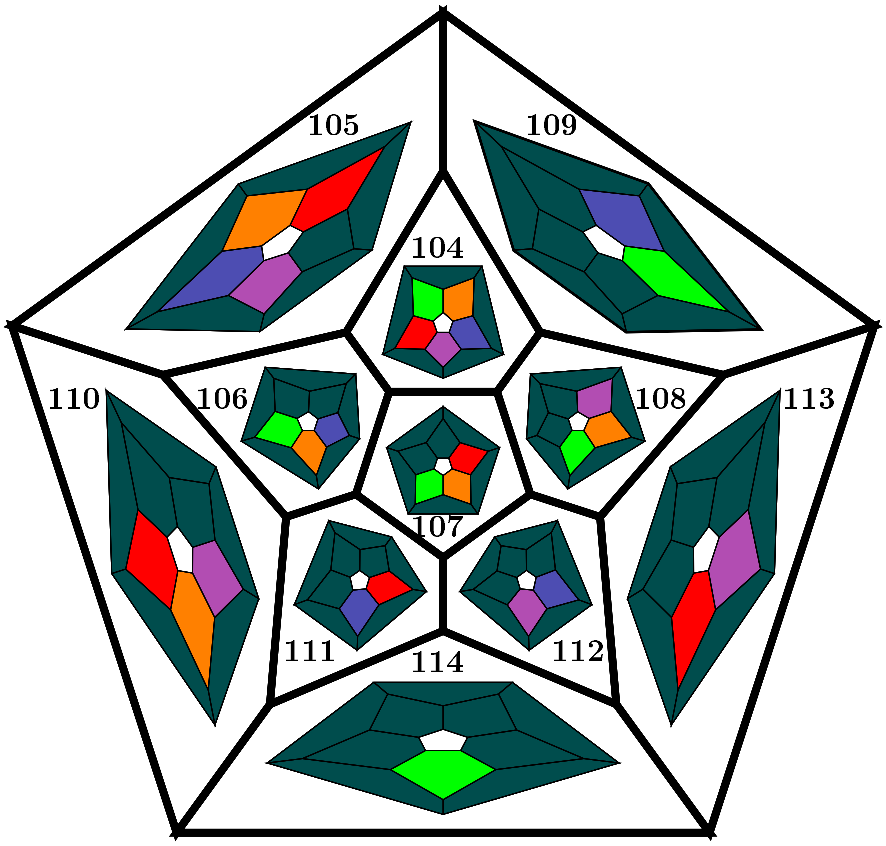

Figure 26. Splitting the basic hyper-corner: the walls being defined by the seventh generation

We number the dodecahedra of the seventh generation from $\mathcal{E}_{104}$ up to $\mathcal{E}_{115}$, following the same ordering as for the previous generations. On the figure 26, $\mathcal{E}_{115}$ is not represented as it lies on the face of the fifth generation which lies on the back of $\mathcal{D}_1$.

We take $\mathcal{E}_{104}$ in order to delimit the first region of the seventh generation. This region is of the type $6a$. It is the single one of this type for this generation. Indeed, from the section 4, in particular from the figure 13 and from the table 11, we know that the dodecahedra of the seventh generation have at most six free faces. As their faces of the inner ring are counted twice for each of them, only the first one can define a region with six faces. The bottom of this new region necessarily defines a wall for the surrounding regions.

This time, we obtain new views of already seen regions. Of course, the six-faced region being associated to $\mathcal{E}_{104}$ corresponds to the right hand picture of the figure 17. For the single five-faced region being defined by $\mathcal{E}_{105}$, we have a new view which is the figure 27.(i). The we have several four-faced and three-faced regions, whose pattern is given, respectively, by the figures 27.(ii) and 27.(iii). The single two-faced region correspond to $\mathcal{E}_{114}$ and the single one-faced region corresponds to $\mathcal{E}_{115}$. The corresponding patterns are give, respectively, by the figures 27.(iv) and 27.(v).

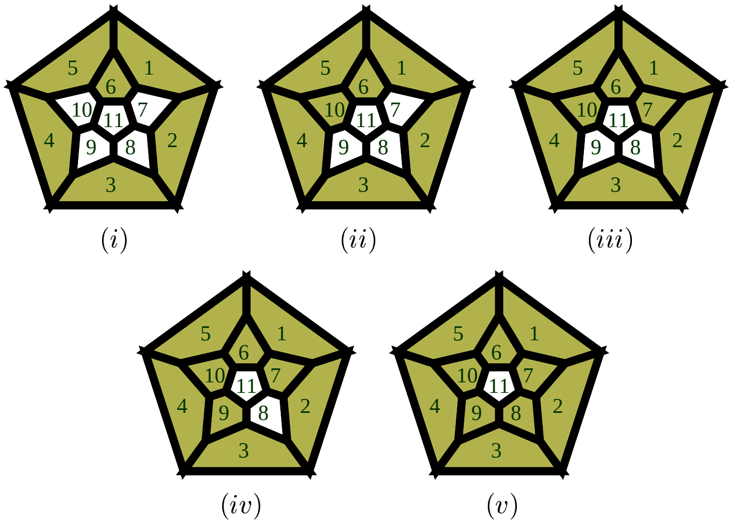

Figure 27. Regions of the seventh generation.

Below, the table 17 gives the contribution of the sixth and seventh generation to the various types of regions of the splitting.

	$6a$	$6b$	5	4	3	2	1
VI	0	1	9	9	1	0	0
VII	1	0	1	4	4	1	1

Table 17. The matrix of the splitting: counting the contribution of the sixth and of the seventh generations.

As a conclusion of the study, we have that the single region of the eighth generation is defined by a dodecahedron with no free face, *i.e.* for which all the orthogonal completions which are constructed on its faces happen to be walls. This case generalises the case of a tunnel which we defined in [14] in the case of $\mathbb{H}^3$.

5.3 The basis of the splitting

In this sub-section, we make an account of the basis of the splitting. In the next section, this will allow us to compute the matrix of the splitting and, consequently, to determine the polynomial of the splitting.

We know that, here, we have only one kind of generating tiles: the rectangular regular dodecahedron. We have to determine the unbounded elements of the basis of the splitting.

In order to do so, we have to justify that the regions which we found in the previous constructions are exactly the regions which enter the basis of the splitting.

Indeed, we have several views of dodecahedra with a given number of shadowed faces, the back being included: from three, up to twelve. As we shall see, we have exactly eleven regions for the basis.

We shall look at all the cases, starting from the nine-faced regions.

Nine- and eight-faced regions

Notice that we met a very small number of nine-faced regions and, in all the cases, we have the same pattern, up to a rotation of the faces around a fixed one.

For the eight-faced regions, there are also a few of them. In our constructions, we found only two different views of them, see the figure 28. Indeed, this two views are different views of the same dodecahedron. We prove this by the numbering of the faces, following the technique which we applied in the construction of the dodecahedra of the second, the fourth, the sixth and the seventh generations. In the figure, faces with the same number in both views are the same.

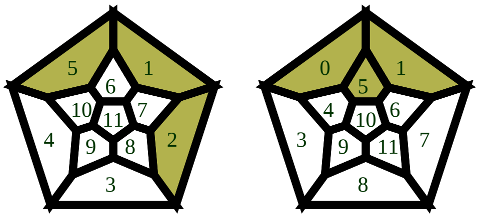

Figure 28. The eight-faced regions are isometric.

Notice that the transformation of the left hand picture into the right hand one consists in turning the dodecahedron around the face 1 in such a way that the face 2 becomes its back. And so, we have isometric regions of $I\!H^4$.

Seven-faced regions

Now, we consider the case of the seven-faced regions. We met such regions in the first, the second and the fourth generations. The figure 29 reminds us all the different view which we found and it proves, by suitable numberings, that all of them are isometric in $I\!H^4$.

Indeed, take as the reference, the picture which is on the upper row, on the left hand. Then, the other picture of the same row is obtained by turning the dodecahedron around the face 1 in such a way that the face 5 becomes the back of the new view, and so the top is now the face 8 and the feet are the face 4. Next, we turn the dodecahedron around its new back in such a way that the feet are the face 10 as it is in the picture of the figure 29.

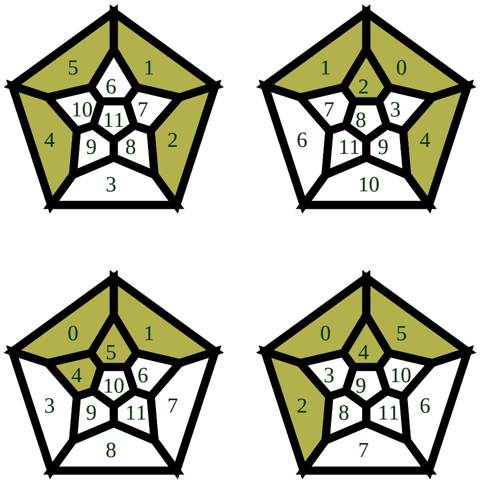

Figure 29. The seven-faced regions are isometric.

Similarly, the picture of the next row and on the left hand is obtained by taking the face 2 as the back and then by rotating the figure around the new back so that the feet are the face 8. At last, the picture of the right hand on the second row is obtained when the back is played by the face 1 and the feet are the face 7 after a suitable rotation around the new back.

The six-faced regions

We have seen four configurations for these regions. Most of them are isometric to the twelve dodecahedra of the third generation which have five shadowed faces around their shadowed back. We found out several copies of another view, especially in the fourth generation. More precisely, this type was found in the first, third, fourth, fifth and seventh generations. We found two views of this type which are given in the figure 30, below.

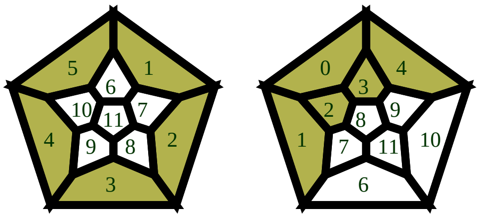

Figure 30. The first kind of regions for the six-faced regions: the type $6.a$.

Here also, the numbering allows us to establish the correspondence between the two views. Indeed, a turn around the face 1 allows us to put the face 5 on the back of the dodecahedron. Then turning it around the face 8 which is the new top, allows us to obtain the right hand part of the figure.

The exceptional case of the fourth generation is a second configuration for the six-faced region. We met this pattern also in the second and in the sixth generation. It is represented below by the figure 31. Recall the simple proof that the patterns are different. Indeed, in the case of the type $6.a$, there is a shadowed face for which all surrounding faces are shadowed. This is not the case in the type $6.b$ where all shadowed faces have at least one un-shadowed neighbour.

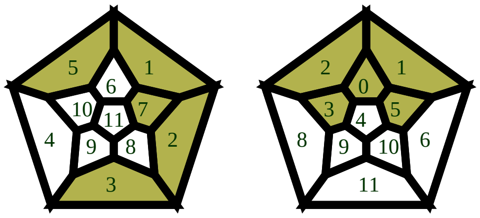

Figure 31. The second kind of regions for the six-faced regions: the type $6.b$.

Notice that the right hand part of the figure 31 is obtained from its left hand part by a turn around the face 1 which puts the face 7 on the back of the dodecahedron.

The five-faced regions

We come now to the five-faced regions which we met during the fourth, the sixth and the seventh generation. All the different views which we encountered are displayed by the figure 32.

We apply the same numbering technique. The basic numbering is given in the figure 32.(i). The figure 32.(ii) is obtained by putting the face 1 as the back of the dodecahedron by a rotation around the face 5. The figure 32.(iii) is obtained by putting the face 10 on the back by a rotation around the face 5 and then, as the face 2 becomes the new top, we rotate the dodecahedron around the face 2 in order to get the configuration being displayed in the figure. In the figure 32.(iv), the rôle of the back is now played by the face 7. It can be obtained from the figure 32.(iii) by the same motion which transforms to the latter one the figure 32.(ii). In the figure 32.(v), the rôle of the back is now played by the face 10. This can be obtained from the figure 32.(i) by the motion being previously considered.

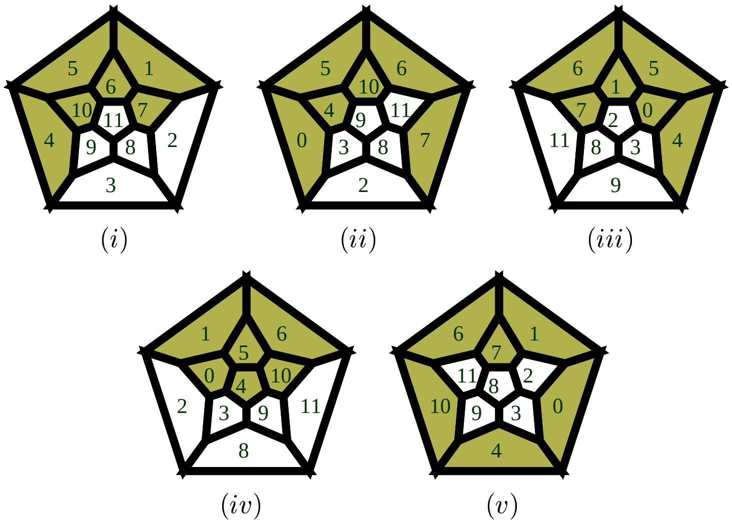

Figure 32. The five-faced regions are isometric.

The four-faced regions

The four-faced regions appear with one sample in the fourth generation and then, in the sixth and in the seventh generations. Three types of views appear, all being isometric as the numbering being displayed by the figure 33 allows us to see.

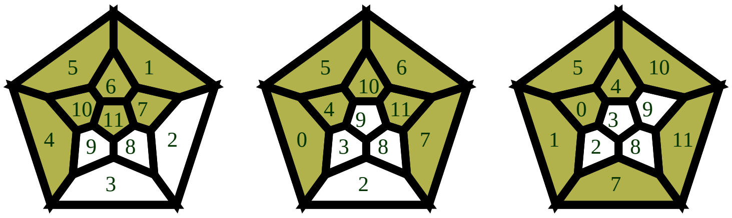

Figure 33. The four-faced regions are isometric.

Here also, the same transformation allows to go from one picture of the figure to the next one, starting from the leftmost one. It is the case for the rotation around the face 5 which puts the face 1 as the back of the new view. In the third view of the figure, rotating the dodecahedron once again around the face 5, the rôle of the back is now played by the face 6.

The three-faced regions

We come to the last case where topologically different views could appear. The views of these regions, which appear in the sixth and seventh generation are displayed in the figure 34. The same rotation as in the four-faced region case allows to go from the left hand picture of the figure to the right hand one.

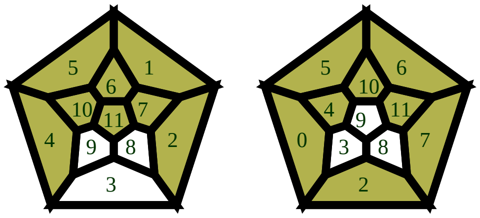

Figure 34. The three-faced regions are isometric.

For what is the two-faced and one-faced regions, they are produced by the seventh generation only. We noticed noticed immediately that there is only one kind of region for each kind, as there is only one region.

5.4 The connection with the dual graph

In order to complete the proof of the correctness of the splitting, we have to see that all 120-cells which share a vertex are reached by the spanning tree of the splitting.

To that purpose, let us go back to what happens with the hyper-cube of $\mathbb{R}^4$: we know that $\mathbb{H}^4$ is locally diffeomorphic to $\mathbb{R}^4$.

Now, looking in $\mathbb{R}^4$ at the hyper-cubes which are around the point $(0,0,0,0)$, we find that if $[0,1]^4$ is taken as the initial hyper-cube, the other ones are obtained as follows, by successive reflections in their hyper-faces:

first generation: four hyper-cubes:
$[0,1]^a \times [-1,0] \times [0,1]^b$ with $a,b \geq 0$ and $a+b=3$;
second generation: six hyper-cubes:
$[0,1]^a \times [-1,0] \times [0,1]^b \times [-1,0] \times [0,1]^c$ with $a,b,c \geq 0$ and $a+b+c=2$;
third generation: four hyper-cubes:
$[-1,0]^a \times [1,0] \times [-1,0]^b$ with $a,b \geq 0$ and $a+b=3$;
fourth generation: one hyper-cube: $[-1,0]^4$.

Indeed, for the first and the second generations, the reader may check that the solutions in natural numbers of $a+b=3$ and $a+b+c=2$ are, respectively:

0	3		0	0	2
1	2		0	1	1
2	1		0	2	0
3	0		1	0	1
			1	1	0
			2	0	0

According to the process which we described in the general tools, in the sub-section 5.1 and in the descriptions of the first generation and of the second one, the same conclusions hold for the 120-cells and their hyper-faces. Notice that, in the above argument, the word 'generation' is taken according to the splitting and not according to the construction of the 120-cell. Notice also that the generations of the splitting corresponds to the number of reflections in hyper-faces which are needed in order to reach a fixed 120-cell, starting from the initial one. We shall go back to this point in the sub-section 6.2.

Notice that analogous situations occur in the cases of $I\!H^2$ and $I\!H^3$.

Indeed, in the case of $I\!H^2$, the four pentagons which lie around a vertex are produced in two generations starting from the initial one. The first generation yields two pentagons and the second generation produces a single one, see, for instance, [12, 6]. The reader may check that we have exactly the same situation with squares in $I\!R^2$.

In the case of $I\!H^3$, the eight dodecahedra which lie around a vertex are produced in three generations, starting from the initial one. The first generation yields three dodecahedra, the second generation also yields three ones. The third generation yields a single one, see [16, 15]. Here also, the reader may check the analogy of the situation with cubes in $I\!R^3$.

6 The algebraic part of the splitting

6.1 The matrix of the splitting

Adding all the information which we got up to now, we can induce the following splitting for the hyper-corner given by the table 18:

	9	8	7	$6a$	$6b$	5	4	3	2	1	0
I	5	0	3	1	0	0	0	0	0	0	0
II	1	9	9	0	1	0	0	0	0	0	0
III	0	0	0	12	0	0	0	0	0	0	0
IV	0	1	9	9	1	9	1	0	0	0	0
V	0	0	0	12	0	0	0	0	0	0	0
VI	0	0	0	0	1	9	9	1	0	0	0
VII	0	0	0	1	0	1	4	4	1	1	0
VIII	0	0	0	0	0	0	0	0	0	0	1
9	6	10	21	35	3	19	14	5	1	1	1

Table 18. The matrix of the splitting: counting the contribution of each generation for the splitting of a hyper-corner.

As it is indicated in the last row of the table 18 by the leftmost number, this table gives us the incident data for a hyper-corner. Recall that a hyper-corner of $I\!H^4$ can be obtained from a dodecahedron by taking three of its faces which share a common vertex and by raising a hyper-plane on each face, perpendicularly to the dodecahedron: together with the considered dodecahedron, this gives us the four walls of the hyper-corner.

As previously, if we distinguish the basic corner, we may represent a hyper-corner by a nine-faced dodecahedron. We met the other types of regions in our previous study and so, we know that there are 11 of them which we can represent by the number of their free faces in the following way:

$$9,\ 8,\ 7,\ 6.a,\ 6.b,\ 5,\ 4,\ 3,\ 2,\ 1,\ 0.$$

The last case of a zero-faced region is provided us by the single dodecahedron of the eighth generation: all its faces are completed when it is appended to the seventh generation. As we already noticed, there are two kinds of six-faced regions. We denote by $6.a$ the case of a dodecahedron of the third generation and we denote by $6.b$ the other case. As we see from the table 18, there are only a few regions of the type $6.b$.

As we notice that we obtain the regions by shadowing the faces of the dodecahedra one after another when we go from one kind of region to the other one. Accordingly, only the contribution of the first generation is modified. It is not the case for the other generations. The splitting of the first generation is given by the pictures of the figure 35, both with and picture and the contribution to the counting for each configuration.

Below, the table 19 takes into account all this information and it gives us the matrix of the splitting.

9	6	10	21	35	3	19	14	5	1	1	1
8	5	10	21	35	3	19	14	5	1	1	1
7	4	10	21	35	3	19	14	5	1	1	1
$6a$	3	11	20	35	3	19	14	5	1	1	1
$6b$	2	12	20	35	3	19	14	5	1	1	1
5	2	11	20	35	3	19	14	5	1	1	1
4	2	10	20	35	3	19	14	5	1	1	1
3	1	11	19	35	3	19	14	5	1	1	1
2	1	10	19	35	3	19	14	5	1	1	1
1	1	10	18	35	3	19	14	5	1	1	1
0	1	10	18	34	3	19	14	5	1	1	1

Table 19. The matrix of the splitting.

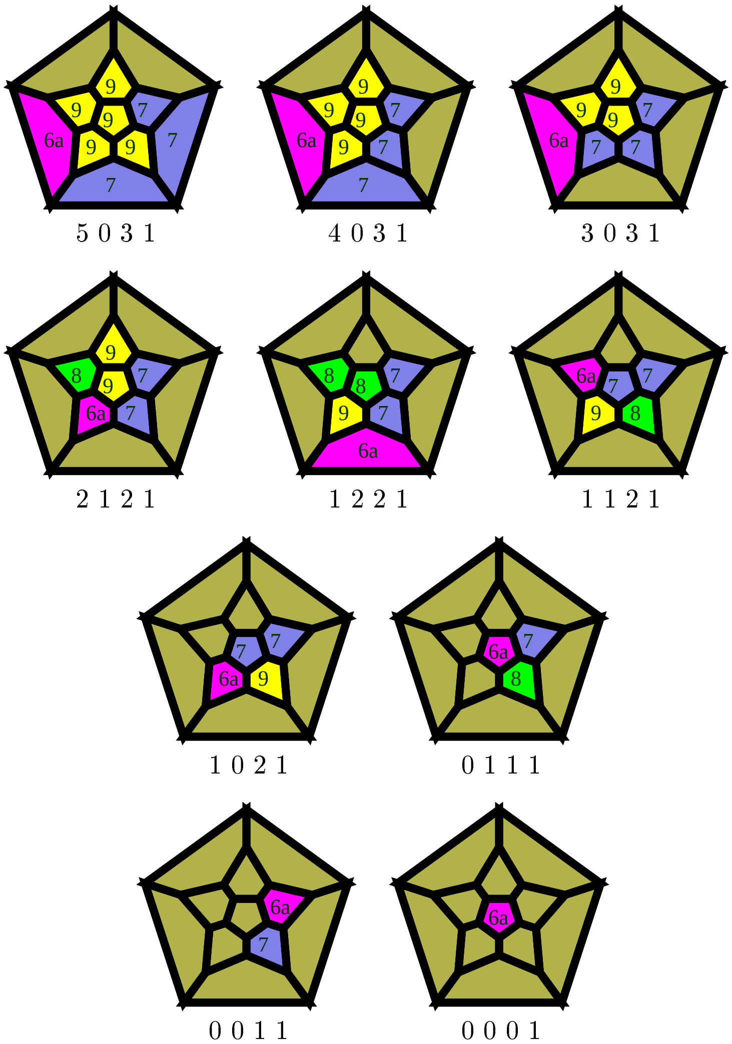

Figure 35. The first generation in the splitting of each kind of region.

6.2 The polynomial of the splitting

The characteristic polynomial of the matrix of the splitting, as being computed by $Maple8$, is the following:

$$P_0(X) = X^{11} - 116X^{10} + 366X^9 - 116X^8 + X^7.$$

Accordingly, the polynomial of the splitting is:

$$P(X) = X^4 - 116X^3 + 366X^2 - 116X + 1.$$

We notice that P is a reciprocal polynomial. As the degree of P is 4, it is possible to express its roots by using square roots of integers. Indeed, it is known that if we set $Y = X + \dfrac{1}{X}$, to solve P boils down to solve a quadratic polynomial. We obtain that $\dfrac{1}{X^2}P(X) = Q(Y)$, where the polynomial Q is given by $Q(Y) = Y^2 - 116Y + 364$. Accordingly, the roots of Q are:

$$Y_1 = 58 + 10\sqrt{30},$$
$$Y_2 = 58 - 10\sqrt{30}.$$

Next, the roots of P are solutions of the equations $x^2 - xY_\alpha + 1 = 0$, with $\alpha \in \{1, 2\}$. Accordingly we obtain:

$$X_1 = \frac{Y_1 + \sqrt{Y_1^2 - 4}}{2}, \qquad X_3 = \frac{Y_2 + \sqrt{Y_2^2 - 4}}{2},$$
$$X_2 = \frac{Y_1 - \sqrt{Y_1^2 - 4}}{2}, \qquad X_4 = \frac{Y_2 - \sqrt{Y_2^2 - 4}}{2}.$$

Replacing Y_1 and Y_2 by the already computed values we obtain:

$$X_1 = 29 + 5\sqrt{30} + \sqrt{1590 + 290\sqrt{30}},$$
$$X_2 = 29 + 5\sqrt{30} - \sqrt{1590 + 290\sqrt{30}},$$
$$X_3 = 29 - 5\sqrt{30} + \sqrt{1590 - 290\sqrt{30}},$$
$$X_4 = 29 - 5\sqrt{30} - \sqrt{1590 - 290\sqrt{30}}.$$

whose approximate values are:

$$X_1 = 112.7633976 \qquad X_3 = 2.880593478$$
$$X_2 = 0.00886813 \qquad X_4 = 0.347150762$$

Now, if $u(0) = 1$, and if we assume $u(-1) = 0$, $u(-2) = 0$ and $u(-3) = 0$, we get, successively:

1	2	3	4	5
116	13 090	1 476 100	166 450 115	18 769 479 064

which are the number of regions of, respectively, the first, the second, the third, the fourth and the fifth generation being obtained by reflections on the hyper-faces of the already constructed 120-cells. Notice that here, the word 'generation' is taken in the context of the tiling. As it is known from [9, 10], the above numbers represent the number of nodes of, respectively, the first, the second, the third, the fourth and the fifth level of the spanning tree of the splitting.

Notice here another interesting analogy with $\mathbb{H}^2$ and $\mathbb{H}^3$. The degree of the polynomial of the splitting is equal to the number of generations which are needed in order to get all the tiles which are around a common vertex.

At this stage, notice that the definition of the sequence $\{u_n\}_{n\in I\!N}$ is an intrinsic property of the **tiling** itself. The notion of generation which corresponds to the level of the spanning tree does not depend on the splitting. In the restriction of the tiling to S_0, the first generation consists of the 116 120-cells which are obtained from the original 120-cell by reflection in its **free** hyper-faces. The second generation is obtained by the **new** 120-cells which are obtained from the original ones with two reflections in hyper-faces: one in a hyper-face of the original 120-cell, the second one in a hyper-face of a 120-cell of the first generation. By induction, the 120-cells of the $n{+}1^{\text{th}}$ generation are obtained by the reflections of the 120-cell of the n^{th} generation which are new 120-cells. Notice that the shadowing rules which we introduced allow us to extract a bijection from the surjection which is induced by the just described process: for some hyper-faces, the reflection in them produces the same 120-cell as we already noticed. Indeed the maximal number of hyper-faces which give raise to the same 120-cell is at most two and so our rule is completely justified. Notice that the proof of this property is based on the fact that four 120-cell occupy the space around a pentagon. The precise characterization of the surjectivity of generating the tiling by reflection of copies of the same 120-cell also indicates that the counting of the new 120-cell of each generation is exactly the number of nodes in the corresponding level of the spanning tree.

6.3 Other bases of splitting

What we just said at the end of the previous paragraph means that if we find another basis of splitting for the splitting, we shall find the same recurrence sequence of the splitting.

In [6], we found infinitely many splittings for the tiling of $I\!H^2$ being generated by the rectangular regular pentagon.

In [14, 15], this question is not mentioned. However, in his personal files, the author examined several possible splittings of the tiling of $I\!H^3$ which is generated by tessellation of the rectangular regular dodecahedron. All of them yield the same recurrent sequence $\{u_n\}_{n\in I\!N}$ of the splitting. Notice that the polynomial of the splitting need not be the same. This well known property is illustrated by the study which we just mentioned.

We shall see here another splitting with a stronger property: it will turn out that the polynomial of the splitting is the same.

Take the splitting of the octant in $I\!H^3$ which is indicated in the figure 18. It gives a significantly different splitting of the octant than the splitting being displayed by the figure 35. Thus, the splitting of the figure 18 yields three octants and four half-octant (eight-faced regions), while the figure 5 yields five octants and no half-octant. If we go on the splitting according to the figure 18 to the other regions, we get the following new matrix being displayed by the table 20.

A simple computation which we checked with *Maple*8 shows us that the polynomial of the new splitting is again the polynomial P given in [15]:

$$P_{I\!H^3}(X) = X^3 - 9X^2 + 9X - 1.$$

	9	8	7	6
3	3	4	1	1
2	2	4	1	1
1	1	4	1	1
0	1	3	1	1

Table 20. The matrix of the splitting for the other splitting of the octant in $I\!H^3$.

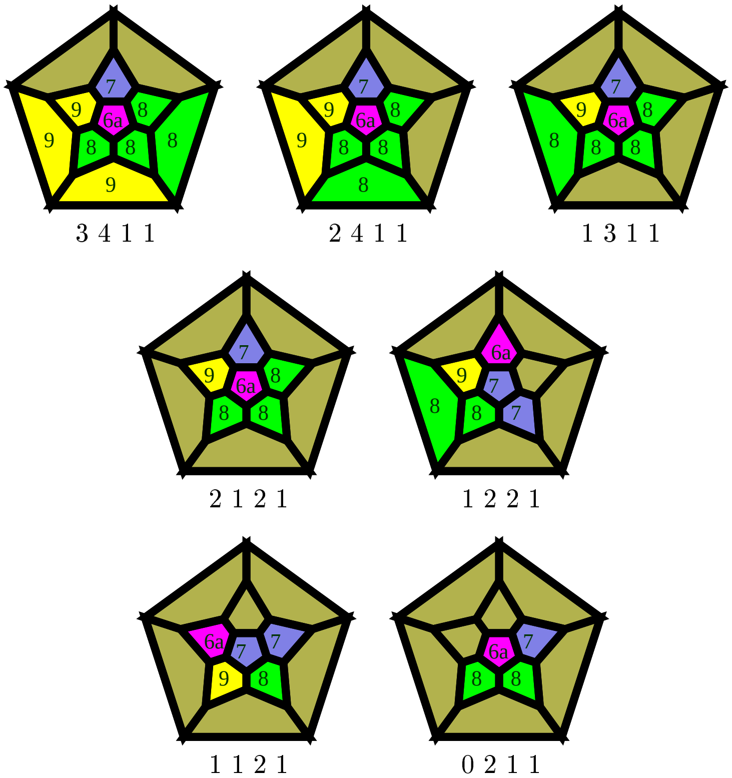

Figure 36. The first generation in the splitting of each kind of region according to the new paradigm.

Let us now turn to the case of the 120-cell tiling in $I\!H^4$. For the first generation, consider that we take the above way of constructing the splitting.

For the hyper-corner and for the first generation, we obtain the splitting of the figure 18. As we need them in the sequel, we give the patterns of the splitting of the other regions in the figure 36.

Starting from the three-faced region, we find again the splitting which is displayed by the figure 35. The indications under the partial figures give the counting of the splitting for the first generation in each kind of region. This has to be added to what we shall find for the other generations, from the second one up to the eighth one.

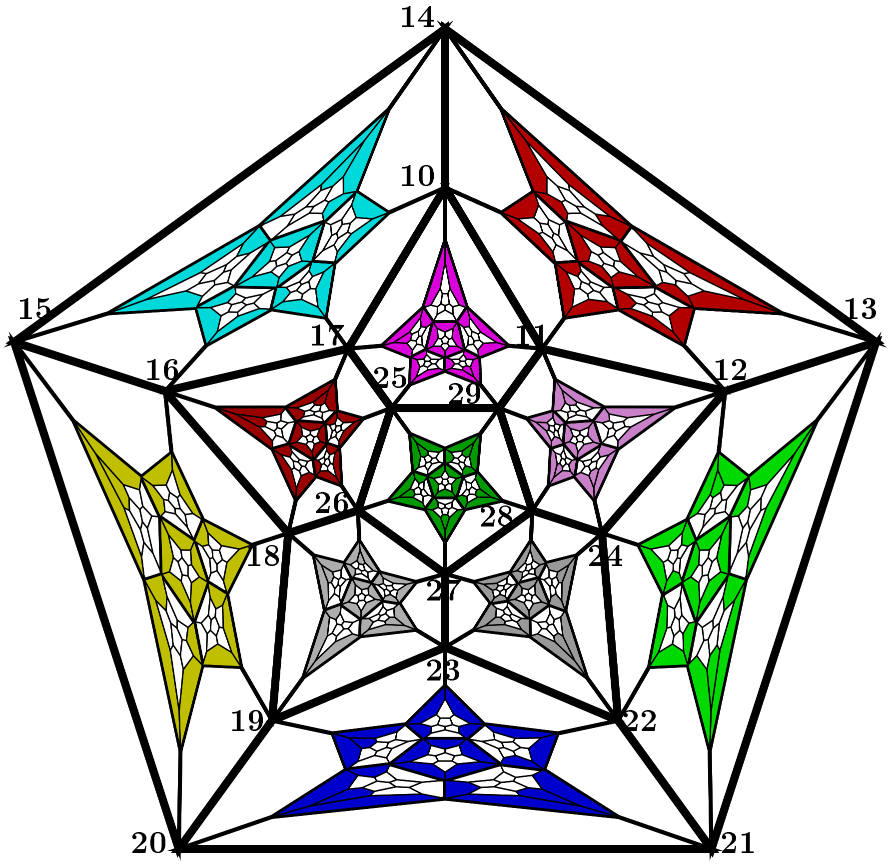

Figure 37. Splitting the basic hyper-corner another way: second and third generation

In what follows, we examine the consequence of following this order of splitting instead of the order which we used in the sub-section 5.2. We notice that, clearly, for the third and for the fifth generation, we have exactly the same results as previously. We shall look only on the second, the fourth, the sixth and the seventh generations. In fact, as we shall see from the figures 37 up to 40, there are no difference in the counting, except for the fourth generation where we find different numbers. Of course, in each generation, the global contribution is the same, whatever the splitting is.

We start with the splitting of the second generation which is displayed by the figure 37. Notice that the numbering of the vertices is not at all the same as in the figure 20. As we already said, this splitting gives the same contribution to each kind of regions as the splitting being displayed by the figure 20: see the table 15.

Next, we turn to the fourth generation which is displayed by the figure 38.

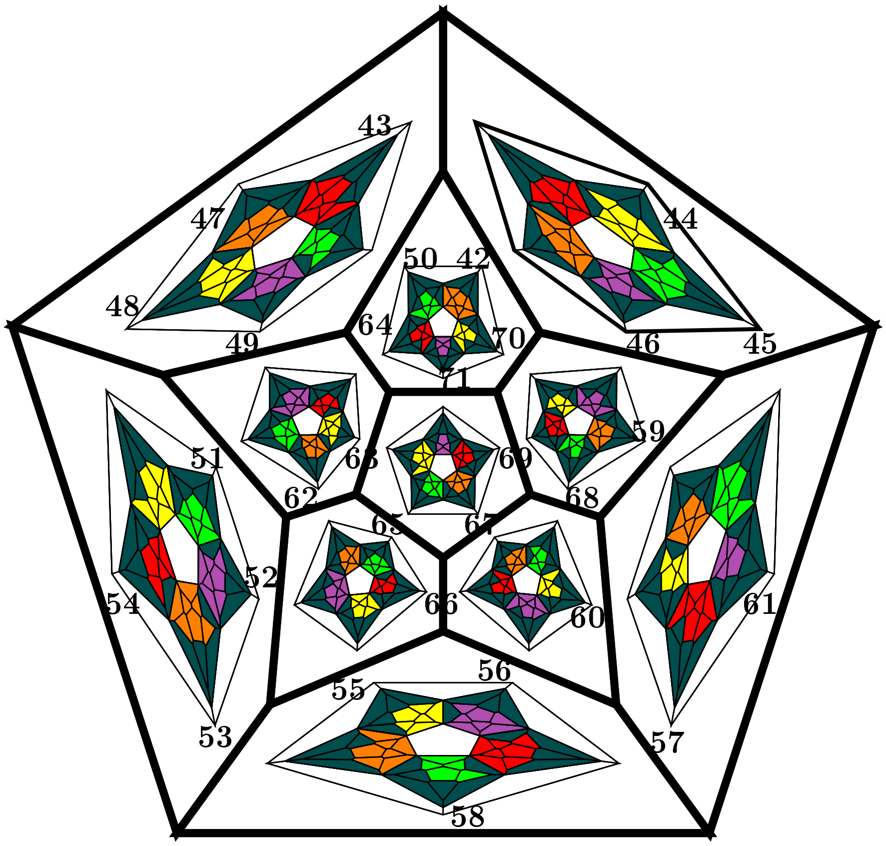

Figure 38. Splitting the basic hyper-corner another way: the walls for the fourth generation

	8	7	$6a$	$6b$	5	4
IV	1	10	8	1	8	2

Table 21. The matrix of the splitting: counting the contribution of the fourth and of the fifth generations.

We notice that, in this case, we have two regions which are four-faced. One appears on the "border" of the figure, see $\mathcal{E}_{61}$, and the other one is the last region being delimited for this generation, $\mathcal{E}_{71}$. Indeed, by the previous numbering, the situations which are distinct in this case happen for the same region, namely for $\mathcal{E}_{71}$. In the previous numbering, $\mathcal{E}_{71}$ is on the "border" of the initial dodecahedron.

And so, we find a different number of four-faced regions. There must be a trade off somewhere else, as long as the global contribution is the same for the whole generation. A careful look at the regions shows that this happens for the seven- and five-faced regions, see the table 21.

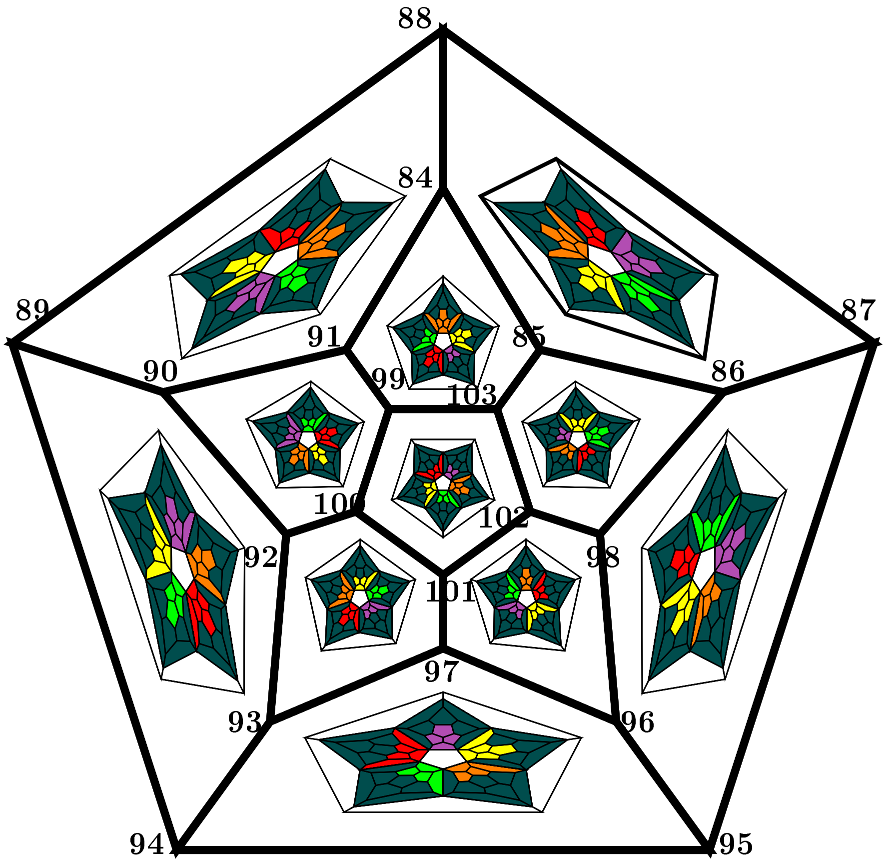

Figure 39. Splitting the basic hyper-corner another way: the walls being defined by the sixth generation

Above, the figure 39 provides us with an illustration of the splitting for the sixth generation. The reader may check by him/her-self that here, we obtain the same contribution to each kind of region as for the splitting being displayed by the figure 22. Notice also that the numbering of the edges in the figure 39 is very different from the numbering of the edges in the figure 22.

We notice also, that in the figure 40 where the seventh generation is displayed, the numbering is very different. There is also a particular situation for this splitting: $\mathcal{E}_{104}$ which is the first region for the seventh generation is put on the back of the initial dodecahedron.

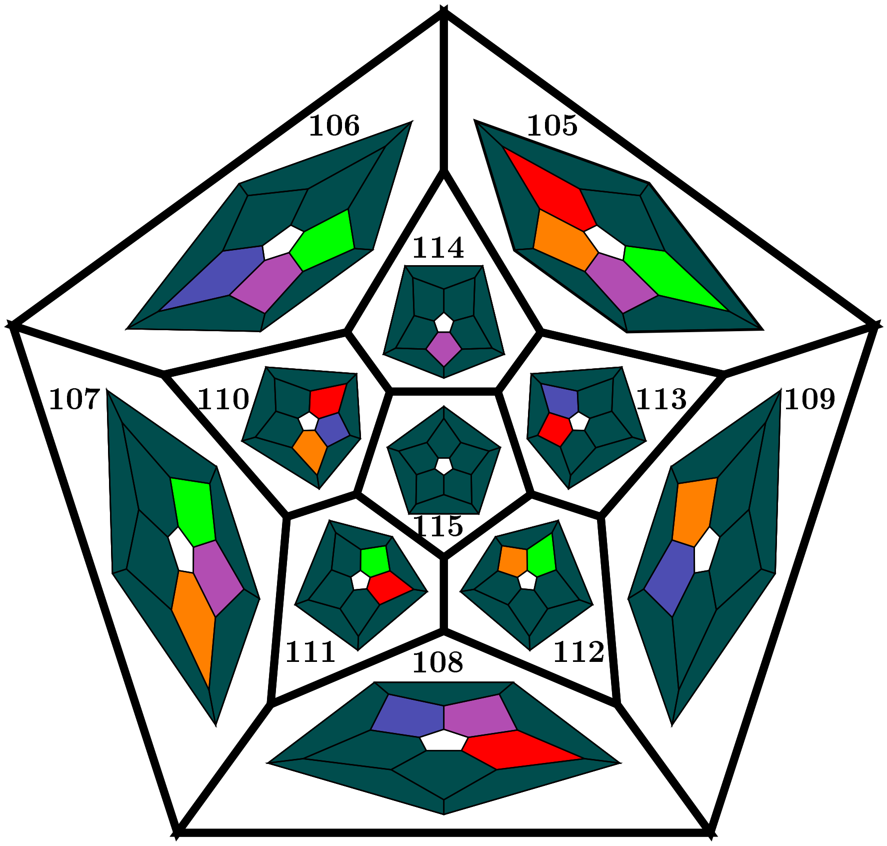

Figure 40. Splitting the basic hyper-corner another way: the walls being defined by the seventh generation; notice that, here, the face 104 is on the back of $\mathcal{D}_1$

Taking into account the various elements which we indicated in the figure 36 and in the table 21, we obtain the counting for the new splitting. The table 22 displays the matrix which corresponds to the new splitting. Notice that the structure of the matrix is very similar to the matrix being displayed by the table 19. Notice also that several values are different.

A computation being performed by *Maple*8 shows us that the characteristic polynomial of this matrix is the same as the characteristic polynomial of the matrix of the table 19.

Notice also that we can mix both splittings. This means that each time when we arrive in a region, we can split it either according to the splitting $\mathcal{A}$ being associated with the matrix of the table 19 or to the splitting $\mathcal{B}$ being associated with the matrix of the table 22. As the spanning tree of the splitting depends on the matrix of the splitting, we obtain the result being stated by the Theorem 3.

	9	8	7	$6a$	$6b$	5	4	3	2	1	0
9	4	14	20	34	3	18	15	5	1	1	1
8	3	14	20	34	3	18	15	5	1	1	1
7	2	14	20	34	3	18	15	5	1	1	1
7	2	14	20	34	3	18	15	5	1	1	1
$6a$	2	13	20	34	3	18	15	5	1	1	1
$6b$	2	12	21	34	3	18	15	5	1	1	1
5	2	11	21	34	3	18	15	5	1	1	1
4	1	12	20	34	3	18	15	5	1	1	1
3	1	11	20	34	3	18	15	5	1	1	1
2	1	10	20	34	3	18	15	5	1	1	1
1	1	10	19	34	3	18	15	5	1	1	1
0	1	10	19	33	3	18	15	5	1	1	1

Table 22. The matrix of the splitting: counting the contribution of each generation for the splitting of a hyper-corner.

Theorem 3 – *There are continuously many spanning trees for the tiling being defined by the tessellation of the* 120*-cell in* $I\!H^4$*, all of them being defined by the same basis of splitting. All of them also yield the same polynomial for the splitting.*

We find here for $I\!H^4$ a property which we proved in $I\!H^2$, with the pentagrid, see [6].

The language of the splitting

As indicated in the section 2, we may associate a language to the splitting. Let $\beta = X_1$, the greatest root of P. We know that we can associate to each positive number n a unique representation in the basis $\{u_n\}$ being defined by the recurrent sequence of the splitting. Indeed n can be represented as follows: $n = \sum\limits_{i=0}^{k} \alpha_i.u_i$ with $\alpha_i \in [0..\lfloor\beta\rfloor]$. For a given representation, define the leading coefficient to be the coefficient α_i with the greatest value of i such that $\alpha_i \neq 0$ and call i the rank of the coefficient. Next, we can make the representation to be unique by taking the representation for which the leading coefficient has the highest rank. Another way to define this representation is to remark that the representation with the leading coefficient of highest rank is also maximal in the lexicographic order being defined on the words with, as letters, the digits in $[0..\lfloor\beta\rfloor]$. The language of the splitting is the set of the $\alpha_k \ldots \alpha_0$'s which are the maximal representations of the positive numbers.

From what we have seen about the roots of P, it is plain that the language of the splitting is not regular, as long as P has two roots which are greater than 1: β and X_3, see [5].

We can sum up all the results which we obtained in the following statement, which is a more precise reformulation of the theorem 2:

Theorem 4 – *The splitting of $\mathbb{H}^4$ which is defined by the tessellation which is generated by the* 120*-cell is combinatoric. Its polynomial is the following one:*

$$P(X) = X^4 - 116\,X^3 + 366\,X^2 - 116\,X + 1,$$

whose greatest root is a Perron number, and the language of the splitting is not regular.

Conclusion

Most probably, there are a lot of properties to find out about the tiling of $\mathbb{H}^4$ being generated to the tessellation of the 120-cell.

As an example, I would like to take the language of the splitting. The language is not regular, this is fixed. Is it context free? I don't know the answer and my feeling is that most probably, it is also not context-free. As far as I could look at this language, it is much more complex than the language of the splitting of $\mathbb{H}^3$ by the rectangular dodecahedron. $\mathcal{L}_{\mathbb{H}^3}$. The proof that $\mathcal{L}_{\mathbb{H}^3}$ is not context-free is greatly facilitated by the structure of the polynomial. In the case of $\mathbb{H}^3$, the presence of the factor $X-1$ in the polynomial entails a lot of cancellations in the computations. This leads to a simple proof of the indicated property of $\mathcal{L}_{\mathbb{H}^3}$. In the case of $\mathbb{H}^4$, the polynomial is reciprocal, but the computations are not that simple.

Indeed, the maximal representation of $u_n - 1$ in the basis being associated to β is not so easy to characterise. The observation seems to give some ground to the following facts.

The representation of $u_n - 1$ can be written, as a word, in the form $b_n e_n$. The beginnings b_n have the property that b_n is also a beginning of b_{n+1}. The ratio between the lengths of b_n and e_n seems to be in favour of b_n and the ratio seems also to be slowly increasing. Indeed, it seems that we have always $|b_{n+1}e_{n+1}| = |b_n e_n| + 1$ and that $|b_{n+1}| - |b_n| \leq 2$. Most often, $|b_{n+1}| - |b_n|$ is 1 and sometime, it is 0.

And so, to elucidate the status of the language of the splitting is not only an open problem. Its solution would probably bring in interesting tools.

Another direction in which this work can be continued is the implementation of cellular automata in $\mathbb{H}^4$. The paper gives a basis for that. In [13, 15], the implementation of cellular automata is dealt with in $\mathbb{H}^3$. At first glance, it seems that the considerations being developed in that paper can be transported to $\mathbb{H}^4$ without major change. In particular, this seems to be the case for the notion of local map which, indeed, can be reduced to the maps for the first level of the tree with all possible kinds of root. The conclusion that the algorithm to locate the neighbours of a cell could be also cubic in the case of $\mathbb{H}^4$ seems to hold too.

References

[1] H. S. M. Coxeter, Regular Complex Polytopes, Cambridge University Press, 1974.

[2] D. B. A. Epstein, J. W. Cannon, D. F. Holt, S. V. F. Levi, M. S. Paterse, W. P. Thurston, Word Processing in Groups, Jones and Barlett Publ., Boston, 1992.

[3] A. S. Fraenkel, Systems of numerations, Amer. Math. Monthly, **92** (1985), 105-114.

[4] D. Hilbert, S. Cohn-Vosen, Geometry and the Imagination, Chelsea Publ. Co, New-York, 1990.

[5] M. Hollander, Greedy numeration systems and regularity, Theory of Comput. Systems, **31** (1998), 111-133.

[6] M. Margenstern, New tools for Cellular Automata in the Hyperbolic Plane, *Journal of Universal Computer Science*, vol **6**, issue 12, 1226–1252, (2000).

[7] Margenstern M., Tiling the hyperbolic plane with a single pentagonal tile, Journal of Universal Computer Science, to appear.

[8] M. Margenstern, A combinatorial approach to infinigons and to infinigrids of the hyperbolic plane, Proceedings of SCI'2002, Orlando, July, 14-18, 2002, (2002).

[9] Margenstern Maurice, A contribution of computer science to the combinatorial approach to hyperbolic geometry, *SCI'*2002, July, 14-19, 2002, Orlando, USA, (2002).

[10] M. Margenstern, Revisiting Poincaré's theorem with the splitting method, talk at **Bolyai'200**, International Conference on Geometry and Topology, Cluj-Napoca, Romania, October, 1-3, 2002.

[11] M. Margenstern, K. Morita, NP problems are tractable in the space of cellular automata in the hyperbolic plane. Technical report, Publications of the I.U.T. of Metz, 38p. 1998.

[12] M. Margenstern, K. Morita, NP-problems are tractable in the space of cellular automata in the hyperbolic plane, *Theoretical Computer Science*, **259**, 99–128, (2001).

[13] M. Margenstern, G. Skordev, Locating cells in regular grids of the hyperbolic plane for cellular automata, Technical report, N° 455, July 2000, Institute für Dynamische System, Fachbereich Mathematik/Informatik/Technomathemtik, Universität Bremen, (2000), 38p.

[14] M. Margenstern, G. Skordev, Tools for devising cellular automata in the 3D hyperbolic space, I - The geometric algorithm, Proceedings of SCI'2002, Orlando, July, 14-18, 2002, (2002).

[15] M. Margenstern, G. Skordev, Tools for devising cellular automata in the 3D hyperbolic space, II - The numeric algorithms, Proceedings of SCI'2002, Orlando, July, 14-18, 2002, (2002).

[16] M. Margenstern, G. Skordev, Tools for devising cellular automata in the 3D hyperbolic space, *Publications du LITA*, N°2002-101, Université de Metz, 52pp., (2002).

available at the following URL: *http://lita.sciences.univ-metz.fr/~margens/*

[17] M. Margenstern, G. Skordev, S. Grigorieff, Two applications of the splitting method: the $3D$ tiling of the rectangular dodecahedra and cellular automata on infinigrids of $\mathbb{H}^2$, Bolyai'2002, János Bolyai Conference on Hyperbolic Geometry, Budapest, July, 8-12, 2002.

[18] H. Meschkowski, Noneuclidean geometry, translated by A. Shenitzer. Academic Press, New-York, 1964.

[19] D.M.Y. Sommerville, An introduction to the geometry of N dimensions, Dover Publ. Inc., New-York, 1958.

[20] J. Stillwell, The Story of the 120-Cell, Notices of the AMS, January 2001.